



doi:10.1016/j.gca.2003.08.015

Mineral dissolution in the Cape Cod aquifer, Massachusetts, USA: I. Reaction stoichiometry and impact of accessory feldspar and glauconite on strontium isotopes, solute concentrations, and REY distribution

MICHAEL BAU,^{1,2,*†} BRIAN ALEXANDER,^{1,†} JOHN T. CHESLEY,³ PETER DULSKI,⁴ and SUSAN L. BRANTLEY¹¹Department of Geosciences, The Pennsylvania State University, University Park, Pennsylvania 16802 USA²Penn State Astrobiology Research Center, The Pennsylvania State University, University Park, Pennsylvania 16802 USA³Department of Geological Sciences, The University of Arizona, Tucson, Arizona 85721 USA⁴GeoForschungsZentrum Potsdam, Telegrafenberg, D-14473 Potsdam, Germany

(Received July 19, 2002; accepted in revised form August 8, 2003)

Abstract—To compare relative reaction rates of mineral dissolution in a mineralogically simple groundwater aquifer, we studied the controls on solute concentrations, Sr isotopes, and rare earth element and yttrium (REY) systematics in the Cape Cod aquifer. This aquifer comprises mostly carbonate-free Pleistocene sediments that are about 90% quartz with minor K-feldspar, plagioclase, glauconite, and Fe-oxides. Silica concentrations and pH in the groundwater increase systematically with increasing depth, while Sr isotopic ratios decrease. No clear relationship between $^{87}\text{Sr}/^{86}\text{Sr}$ and Sr concentration is observed. At all depths, the $^{87}\text{Sr}/^{86}\text{Sr}$ ratio of the groundwater is considerably lower than the Sr isotopic ratio of the bulk sediment or its K-feldspar component, but similar to that of a plagioclase-rich accessory separate obtained from the sediment. The Si- $^{87}\text{Sr}/^{86}\text{Sr}$ -depth relationships are consistent with dissolution of accessory plagioclase. In addition, solutes such as Sr, Ca, and particularly K show concentration spikes superimposed on their respective general trends. The K-Sr- $^{87}\text{Sr}/^{86}\text{Sr}$ systematics suggests that accessory glauconite is another major solute source to Cape Cod groundwater. Although the authigenic glauconite in the Cape Cod sediment is rich in Rb, it is low in in-grown radiogenic ^{87}Sr because of its young Pleistocene age. The low $^{87}\text{Sr}/^{86}\text{Sr}$ ratios are consistent with equilibration of glauconite with seawater. The impact of glauconite is inferred to vary due to its variable abundance in the sediments. In the Cape Cod groundwater, the variation of REY concentrations with sampling depth resembles that of K and Rb, but differs from that of Ca and Sr. Shale-normalized REY patterns are light REY depleted, show negative Ce anomalies and super-chondritic Y/Ho ratios, but no Eu anomalies. REY input from feldspar, therefore, is insignificant compared to input from a K-Rb-bearing phase, inferred to be glauconite. These results emphasize that interpretation of groundwater chemistry, even in relatively simple aquifers, may be complicated by solute contributions from “exotic” accessory minerals such as glauconite. To detect such peculiarities, groundwater studies should combine the study of elemental concentration and isotopic composition of several solutes that show different geochemical behavior. Copyright © 2004 Elsevier Ltd

1. INTRODUCTION

Radiogenic isotope ratios, particularly those of Sr, have been used to determine groundwater flow paths, weathering rates, mixing relationships, groundwater ages, and other aspects of water-rock interaction (e.g., Åberg et al., 1989; Blum et al., 1993; Miller et al., 1993; Bullen et al., 1996; Bullen et al., 1997; Clow et al., 1997; Johnson and DePaolo, 1997; Johnson et al., 2000; Probst et al., 2000; Aubert et al., 2001; Millot et al., 2002, and references therein). In groundwater studies, Sr isotopic data are often preferred over Sr concentration data. Strontium concentrations are controlled by Sr input via dissolution, desorption or ion exchange, and Sr loss resulting from precipitation and sorption. In contrast, Sr isotopic ratios are only affected by Sr input, because there is no fractionation of ^{87}Sr from ^{86}Sr during Sr removal processes. Hence, the $^{87}\text{Sr}/^{86}\text{Sr}$ ratio of groundwater largely reflects that of the minerals from

which the Sr originates. Since ^{87}Sr forms by radioactive decay of ^{87}Rb , the $^{87}\text{Sr}/^{86}\text{Sr}$ ratio of Rb-bearing minerals in a rock, sediment or soil increases with time at a rate that depends on the initial $^{87}\text{Rb}/^{86}\text{Sr}$ ratio. Strontium released from different minerals during weathering is, therefore, characterized by a mineral-specific isotopic composition. Early studies often related the $^{87}\text{Sr}/^{86}\text{Sr}$ ratio in groundwaters (and river waters) to silicate-weathering (e.g., Blum et al., 1993) with emphasis on biotite or feldspar weathering. Recent investigations have highlighted Sr contributions from (accessory) carbonates (e.g., Clow et al., 1997; Quade et al., 1997; Blum et al., 1998; English et al., 2000; Jacobson and Blum, 2000).

Over the recent years, rare earth element (REE) studies or combined rare earth yttrium (REY) studies of groundwater have similarly gained momentum (e.g., Johannesson and Hendry, 2000, and references therein). However, most studies are qualitative except for recent work such as the utilization of anthropogenic Gd anomalies in REE patterns as a hydrochemical tracer (Möller et al., 2000). Extending REY groundwater studies to include Nd isotopes is promising (e.g., Möller et al., 1998; Tricca et al., 1999; Negrel et al., 2000; Aubert et al., 2001), but compared to Nd isotopic data for hydrothermal

* Address reprint requests to Michael Bau, Geosciences and Astrophysics, International University Bremen, P.O. Box 750561, D-28725 Bremen, Germany (m.bau@iu-bremen.de).

† present address: Geosciences and Astrophysics, International University Bremen, P.O. Box 750561, D-28725 Bremen, Germany

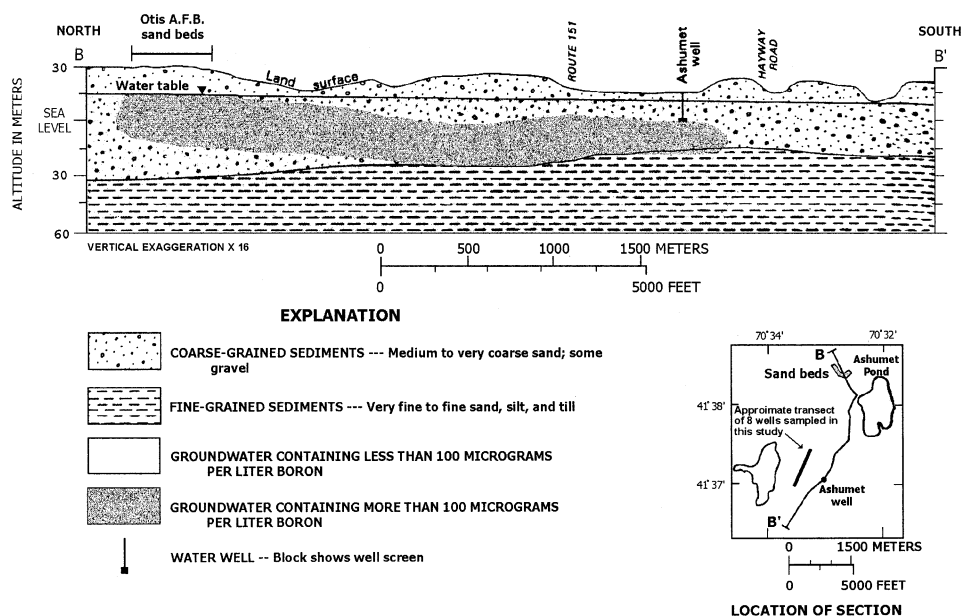


Fig. 1. Location of study area and cross-section of Cape Cod aquifer showing sediment type, contaminant plume, and an approximate transect of MLS wells sampled for this study (modified after LeBlanc, 1984).

fluids, such data are rare. Hence, little is known about which minerals are the main source of REY in groundwater and about the relative importance of input mechanisms, such as desorption, mineral dissolution, and ion exchange. The trivalent REY show coherent behavior during geochemical processes due to their identical valencies and the systematic decrease of ionic radii with increasing atomic number, leading to predictable fractionation trends. Radius-dependent fractionation of light from heavy REE (LREE and HREE, respectively) may occur during incorporation into crystal lattices and during sorption. Fractionation of the only redox-sensitive REY, Ce and Eu, from the non-redox sensitive REY may result from the formation of Ce(IV) or Eu(II) compounds, and solution- and surface-complexation may cause fractionation of Y from Ho, and of La, Gd and possibly Lu from their respective neighbors in the REY series. In contrast to “conservative” Sr, the REY are particle-reactive and their residence times in groundwater, like those in seawater, should be considerably shorter than that of Sr. This suggests that the information gleaned from the REY may complement information from Sr.

Here, we report results of a study of the controls on solute concentrations and on the isotopic composition of Sr in groundwater from a shallow aquifer with unconsolidated, glaciogenic Pleistocene sediment on the Cape Cod peninsula, Mass., USA. Such unconsolidated glacial aquifers are widespread and of great importance, because water supplies for many metropolitan areas are derived from such aquifers. In addition, the groundwater flow, the groundwater chemistry, and also the sediment mineralogy at Cape Cod have been thoroughly and extensively investigated (e.g., Barber, 1985; LeBlanc et al., 1991; Barber et al., 1992; Coston et al., 1995; Masterson et al., 1996; DeSimone et al., 1997; Savoie and LeBlanc, 1998; Yau, 1999; Shapiro et al., 1999; and references therein). This site represents a relatively simple aquifer—a best case aquifer wherein analysis of mineral dissolution was anticipated to be

unequivocal and where the hydrology was well-understood. Specifically, it was anticipated that, since the aquifer is sand and gravel consisting of 95% (wt.) quartz and feldspar (Barber et al., 1992; Coston et al., 1995), and less than 1% silt and clay and less than 0.1% organic carbon (Barber et al., 1992), dissolution reactions could be easily interpreted.

However, we will show that interpretation of mineral reactions is only possible using a combination of major and trace elements and Sr isotopes. We show for the Cape Cod aquifer that dissolution of accessory plagioclase controls Si release and exerts an important control on $^{87}\text{Sr}/^{86}\text{Sr}$ while dissolution of K-feldspar is insignificant. This simple picture is complicated, however, by the additional release of Sr and K (and other solutes) via Si-conservative alteration of authigenic glauconite that occurs as an accessory component in the sediment. Glauconite dissolution particularly impacts groundwater composition in the shallow part of the aquifer. However, this Sr input is only apparent in solute concentrations, but is not observed in the Sr isotopic data, presumably because the Sr released from glauconite is isotopically similar to the plagioclase Sr. The REY distribution in Cape Cod groundwater suggests that the REY are derived from glauconite or other accessory minerals and that feldspar dissolution is insignificant for the REY budget and does not affect the REY patterns of this groundwater. The complicated path of release in this simple aquifer points to the fact that interpretation of water-rock interaction must rely on multiple geochemical tracers to elucidate mineral reactivity.

2. STUDY SITE AND METHODS

2.1. Study Site

The study site is located in the Ashumet Valley, northeastern Falmouth, Cape Cod, Massachusetts, USA (Fig. 1). Operations at Cape Cod’s Massachusetts Military Reservation (MMR) resulted in severe contamination of the groundwater via infiltration beds into the underlying aquifer from the MMR towards Vineyard Sound. To determine

the nature and extent of the contaminant plume, the United States Geological Survey (USGS) installed 315 observation wells and 31 multi-level sampling wells (Savoie and LeBlanc, 1998). Hence, this part of the Cape Cod aquifer has become one of the best-described aquifers in the world.

2.2. Water Samples

Forty-six groundwater samples were collected on June 5th and 6th, 1997, from eight multilevel sampling (MLS) wells installed by the USGS (using hollow-stem-auger drilling and allowing natural collapse of the aquifer material around 1.25-inch diameter PVC casing, Savoie and LeBlanc, 1998). Each MLS well consists of 15 polyethylene tubes (0.25-inch outer diameter) that extend from the land surface into the aquifer material through holes drilled in the well casing at various depths. The open bottom end of each polyethylene tube (the sampling port) is screened with nylon fabric.

The eight MLS wells (262, 508, 373, 168, 442, 471, 472, 350) were chosen because they form a ~900 m long transect (Fig. 1) that roughly parallels the groundwater flow path. Based on published information about specific conductance and concentrations of MBAS (methylene blue active substance) and boron (LeBlanc, 1984; Thurman et al., 1986; Savoie and LeBlanc, 1998), we designed our sampling strategy to ensure that our samples originate from above the contaminant plume. This was later tested and verified by data for specific conductance and boron concentration in our groundwater samples (Appendix 1), that are well below the high values typical of the plume. Due to the almost horizontal groundwater flow (e.g., LeBlanc et al., 1991) the age of the groundwater increases with sampling depth. This has recently been re-confirmed by ³H-³He dating (Shapiro et al., 1999), indicating that in well #350, for example, the groundwater age above the contaminant plume increases downward over a vertical distance of ~12 m from 0.6 ± 0.7 yrs close to the surface of the water table to 14.8 ± 0.6 yrs. The average interstitial velocity of the groundwater flow within the plume is as high as 126 m yr⁻¹ due to the point-source recharge from the infiltration beds (Shapiro et al., 1999). Without this additional recharge, the velocity above the plume (where our samples derive) is considerably slower and probably similar to the 20 to 90 m yr⁻¹ flow rate determined for a nearby site with similar sediment that receives uniform areal recharge (Solomon et al., 1995).

Samples were extracted from the wells with a GeoPump2 peristaltic suction pump connected directly to polyethylene tubes with Norprene tubing. A minimum of three tubing volumes were withdrawn (~ 1.5 L) before sample collection. A 0.45 μm filter was connected to the tubing and acid-cleaned sample bottles were filled after rinsing twice. Samples for cation analyses were acidified in the lab with 1 mL concentrated ultrapure nitric acid/100 mL sample.

Alkalinity was measured in the field during sample collection, using a Hach digital titrator model 16900. Anion concentrations (NO₃⁻, SO₄²⁻, and Cl⁻) were determined with a Dionex DX-100 ion-chromatograph.

Groundwater samples were analyzed for Na, K, Ca, Mg, Si, Al, Fe, and Mn using a Leeman Labs PS3000UV inductively coupled plasma spectrophotometer (ICP-AES) in the Materials Characterization Laboratory (MCL) at Penn State. Boron analyses were conducted at the MCL using a Finnigan Element 1 High Resolution Magnetic Sector ICP-MS. Strontium concentrations were determined with a Turner Scientific quadrupole TS-Sola ICP-MS at University of Arizona. For six samples from well #373, Rb, Sr, Y, Ba, and U concentrations were measured with a Perkin-Elmer Elan 5000 ICP-MS at GFZ Potsdam, Germany. Concentrations of Y and REE in these samples were also determined by ICP-MS at GFZ Potsdam, Germany, but required a separation and preconcentration procedure (for methodical details including precision and accuracy see Bau and Dulski (1996)). The REY distribution patterns are presented normalized to C1-chondrite (subscript 'CN', chondrite from Anders and Grevesse (1989)) or post-Archean Australian Shale, PAAS (subscript 'SN', PAAS from McLennan (1989)). REY data for Cape Cod groundwater has also been normalized to bulk aquifer sediment. In all REY patterns, Y is inserted between Dy and Ho according to its ionic radius. Normalized Ce and Eu anomalies are quantified as $Ce_N/Ce_N^* = Ce_N/(0.5La_N + 0.5Pr_N)$ and $Eu_N/Eu_N^* = Eu_N/(0.5Sm_N + 0.5Gd_N)$, respectively.

Strontium isotopic ratios of groundwater samples and of solutions from sequential leaching of aquifer sediment were analyzed at Univer-

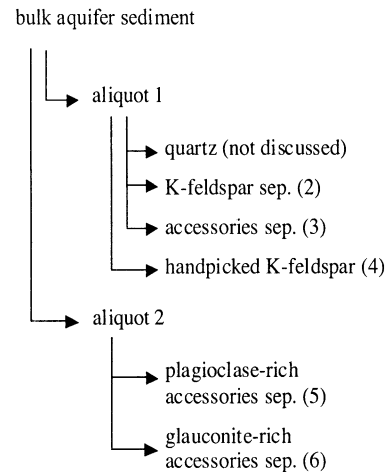


Fig. 2. Flow chart diagram illustrating relationships between bulk aquifer sample and mineral separates obtained from it.

sity of Arizona with a Fisons Sector 54 multi-collector thermal ionization mass spectrometer (TIMS) in multi dynamic mode. All isotopic composition and concentration measurements were determined on spiked aliquots of sample using a 99.9% ⁸⁴Sr spike. Leachates and waters were spiked and allowed to equilibrate for 24 h. Mineral separates were spiked and dissolved in HF+HNO₃ for 24 h, then dried in a HEPA-filtered environment. The sample was then dissolved in 6 mol/L HCl for 24 h, dried, and redissolved in 8 mol/L HNO₃. Sr was separated utilizing Sr Spec resin (Eichrome Industries). Samples were loaded on tantalum filaments with Ta gel to enhance ionization (R. A. Creaser, private communication). Analyses of NBS-987 performed during the study yielded a reproducibility of 0.710251 ± 0.000004 (*n* = 4). The ⁸⁷Sr/⁸⁶Sr ratio is corrected for fractionation using an ⁸⁸Sr/⁸⁶Sr ratio of 0.1194.

2.3. Sediment Samples

The Cape Cod aquifer sediments have been meticulously investigated by many authors in the past (e.g., Barber, 1985; Barber et al., 1992; Coston et al., 1995; DeSimone et al., 1997) and hence, we did not re-do this extensive analysis.

The Cape Cod aquifer consists of boulders, gravel, sand, silt, and clay deposited during the retreat of Pleistocene ice sheets (Oldale, 1969). Sediments were deposited as moraines, basal till, and pro-glacial lake deposits. The sediment within the study area is stratified glacial outwash consisting primarily of unconsolidated medium-coarse sand with some gravel and underlain by fine sand and silt (Barber, 1985; Coston et al., 1995; Masterson et al., 1996). Median grain size (by weight) is approximately 0.5 mm, silt-sized and clay-sized particles comprise less than 1 wt.% of the sediment, and sedimentary organic carbon represents <0.1 wt.% (Barber et al., 1992). Quartz dominates (90–95 wt.%) the <1 mm fraction, while feldspar represents ~5% (wt.) of the <1mm size fraction (Coston et al., 1995). Plagioclase predominates the feldspar fraction (Barber, 1985) and DeSimone et al. (1997) report a plagioclase/K-feldspar weight ratio of 1.5 for the sand and silt-sized fraction of the aquifer sediment.

For this study several mineral separates were prepared for major and trace element and isotope analysis (Fig. 2). The aquifer sediment samples were collected with a wireline piston coring device by the USGS in 1988 from the uncontaminated part of the aquifer at a depth of 13 m above mean sea level, and were frozen for storage. The sampling site was 2 m east of row 12 indicated in Figure 2 of Kent et al. (1994). Sampling location lies between Ashumet pond and the Otis air base sewage infiltration beds. Thawed samples were air-dried in a laminar flow hood and sieved with a 1 mm polyethylene screen (bulk sediment sample, 1 in Table 1).

From 50 g of the <1 mm fraction, three subfractions were separated by heavy liquid separation using bromoform and acetone: a quartz

Table 1. XRF analyses (wt%) of bulk aquifer sediment and selected mineral separates (analyses performed by XRAL Laboratories, Ann Arbor, MI).

	Bulk sediment (1)	"K-feldspar" separate (2)	"Accessories" separate (3)
SiO ₂	95.5	72.7	59.7
Al ₂ O ₃	1.90	14.3	18.4
CaO	0.06	0.09	1.37
MgO	<0.01	<0.01	1.74
Na ₂ O	0.26	2.47	2.14
K ₂ O	0.61	8.42	2.60
Fe ₂ O ₃	0.62	0.43	9.60
MnO	<0.01	0.01	0.14
TiO ₂	0.11	0.06	0.89
P ₂ O ₅	0.02	0.04	0.18
LOI	0.38	0.55	3.23

XRF = X-ray fluorescence

fraction (not discussed further), a "K-feldspar separate" (2 in Table 1), and an "accessories separate" fraction (3 in Table 1). Major element concentrations were determined on these fractions using X-ray fluorescence (XRF, Table 1) and individual mineral grains from separates were studied in polished grain mounts using a Cameca SX-50 electron microprobe. Trace element concentrations in mineral separates and bulk sediment were determined by ICP-MS at GFZ Potsdam, Germany, following decomposition in HF+HClO₄ and HCl in pressure vessels (precision and accuracy are considerably better than ±10%; for details see Dulski (1994)).

Sequential leaching (following the approach of Tessier et al. (1979)) was conducted on the <1 mm fraction of the aquifer sediment (bulk sediment, Table 1) to determine the isotopic composition of the "exchangeable" Sr, the "carbonate" Sr, and the "Fe-Mn oxide-bound" Sr. Here, "exchangeable" Sr was leached from the aquifer sediment using a 1 mol/L sodium acetate (NaOAc) solution of pH 8.86 at room temperature. After agitating the sediment and NaOAc for 1 h, the sample was centrifuged for 30 min at 4200 rpm and the supernatant was decanted. Between each successive extraction deionized water was added to the sample and the sediment was centrifuged for 30 min (4200 rpm), after which this supernatant was discarded. The "carbonate extraction" was performed with 1 mol/L NaOAc titrated to a pH of 5.01 with acetic acid (HOAc). The sediment was agitated for 3 h at room temperature, and a supernatant was collected following the procedure for the exchangeable fraction. Strontium bound to Fe-Mn oxides was leached from the sediment with 0.04 mol/L hydroxylamine hydrochloride in 25% (v/v) acetic acid. This extraction was performed at ~96°C with occasional agitation for four hours, and the supernatant was collected as above. Note that the terms "exchangeable" and "carbonate" are used following Tessier et al. (1979) and do not necessarily imply that only exchangeable and carbonate bound elements were dissolved.

3. RESULTS

3.1. Groundwater

Considering that groundwater flow in the Ashumet Valley is almost horizontal and that it is difficult to assess accurate flow lines, we attempted in earlier work (Yau, 1999) to calculate flow lines and determine changes in Si concentration along flow paths based upon different assumptions and using a larger dataset of wells. For all flow paths, slight increases in Si concentration were observed. However, hydraulic conductivity in the aquifer ranges over one order of magnitude (LeBlanc et al., 1991) and the horizontal/vertical conductivity ratio varies between 2 and 5 (Masterson et al., 1996) due to lenses and layers of coarse grained sediment. Hence, actual groundwater pathways in the upper part of the Cape Cod aquifer we sampled

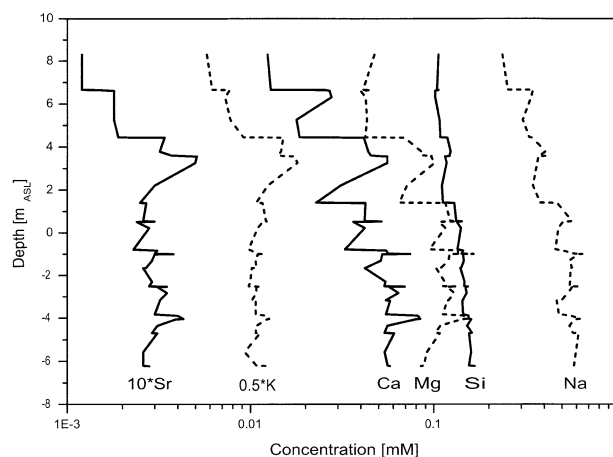


Fig. 3. Graphs of dissolved solute concentrations vs. depth for groundwater from Cape Cod. The trend lines are 3-point moving averages of groundwater concentrations determined from 46 samples from 8 wells (Appendix 2); "depth" is depth relative to average sea level (ASL). Note systematic increase of [Si] and concentration spikes of Sr, K, Mg, and Ca, at about +3 m depth.

show relatively wide small-scale variability. Therefore, inaccuracy in designation of flow path and lack of concentration data for all of the wells lead us to follow mineral reaction utilizing a different approach. Shapiro et al. (1999) used tritium ages to document that the age of groundwater increases with depth in the Cape Cod aquifer. The change in concentration as a function of age (or time in the subsurface) is therefore best assessed by analyzing change in concentration as a function of depth. Thus, we combined data for all samples from all wells and calculated 3-point moving averages to quantify variation of solute concentrations with depth (Fig. 3). "Depth" in this paper refers to the depth relative to average sea level (ASL).

Solute concentrations reported here are similar to values reported by the USGS (Savoie and LeBlanc, 1998) for the same wells and generally increase with depth. For example, Si concentrations increase with depth from 95.4 to 182 μ M (Fig. 4a). Concentrations of Na, K, Ca, and Sr also increase with depth (Figs. 3 and 4). For most solutes (with the notable exception of Si and to some extent Na) the increase of concentration with depth is more pronounced in the shallow than the deeper part of the aquifer (Fig. 4). A spike of Sr, Ca, and K concentration (Figs. 3 and 4) is particularly noticeable at ca. +3 m depth; this spike does not show up in the Si and Na profiles (Figs. 3 and 4). The size of this spike varies between individual wells. However, concentration data for groundwater sampled by the USGS in December 1994 at the same ports from the same wells show similar trends including the +3 m spike (Savoie and LeBlanc, 1998).

We emphasize that because of the near horizontal groundwater flow, a decreasing solute concentration with increasing depth does *not necessarily* indicate loss of that solute (due to precipitation or sorption, for example) but rather indicates flow paths with variable sources of that cation.

Sr concentrations correlate positively with K concentrations (Fig. 5) and this trend is somewhat clearer in the shallow than in the deeper part of the aquifer. Ca/Sr molar ratios increase with depth (Fig. 4c).

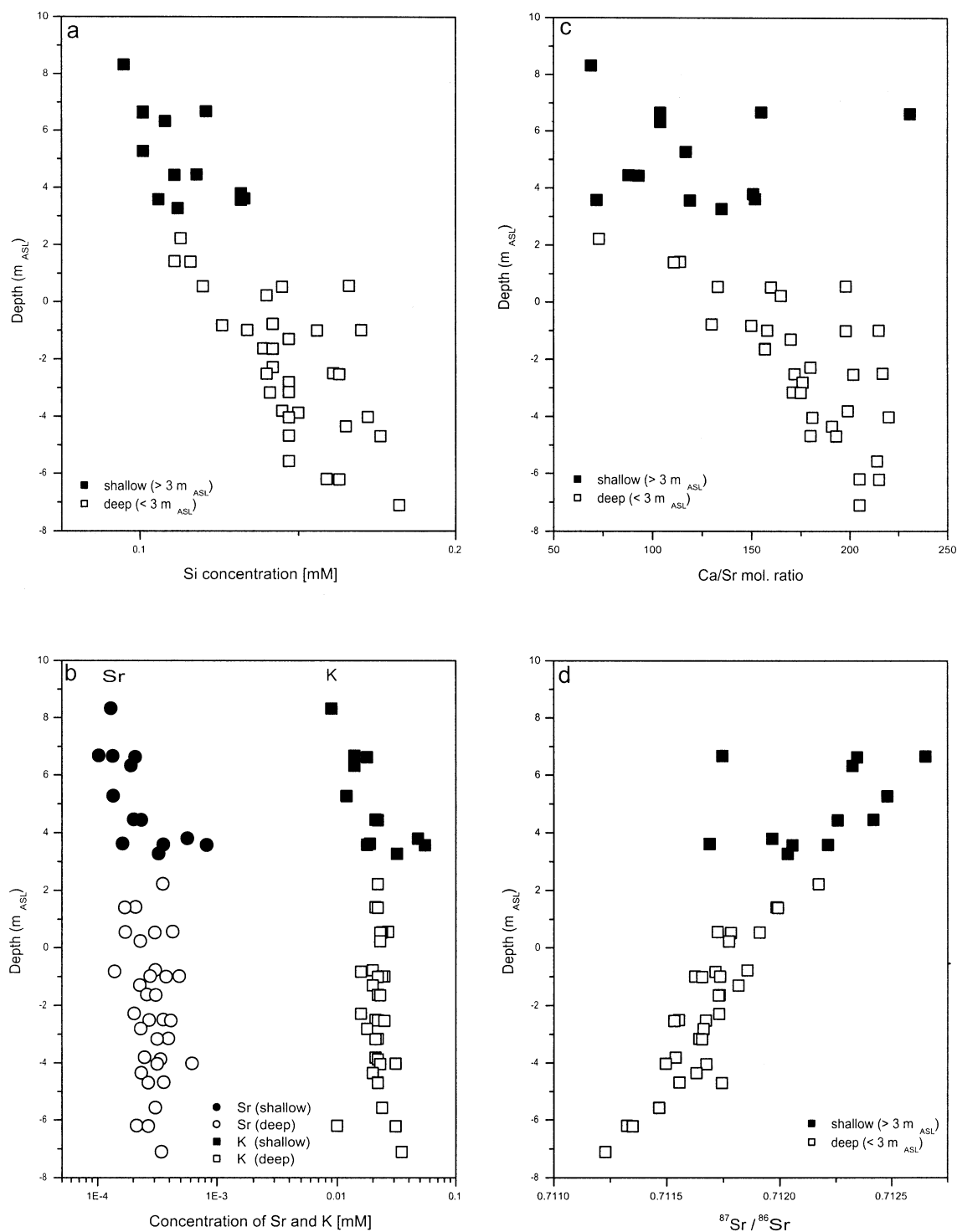


Fig. 4. Graphs of all data points for all wells for dissolved a) Si vs. depth, b) K and Sr vs. depth, c) Ca/Sr molar ratio vs. depth, and d) $^{87}\text{Sr}/^{86}\text{Sr}$ vs. depth.

$^{87}\text{Sr}/^{86}\text{Sr}$ ratios (0.7112302–0.7126519, Appendix 2) decrease systematically with depth and, similar to Ca/Sr ratios, the range of $^{87}\text{Sr}/^{86}\text{Sr}$ ratios in the shallow part exceeds that in the deeper part (Fig. 4d). The +3 m spike seen for K and Sr concentrations is reflected in the $^{87}\text{Sr}/^{86}\text{Sr}$ vs. depth plot in a decreased $^{87}\text{Sr}/^{86}\text{Sr}$ ratio (Fig. 4d). While Sr concentration and

$^{87}\text{Sr}/^{86}\text{Sr}$ ratios are negatively correlated in the shallow part, these two show little correlation in the deeper part (Fig. 6a). A similar relationship exists between $^{87}\text{Sr}/^{86}\text{Sr}$ and K (Fig. 6b). Moreover $^{87}\text{Sr}/^{86}\text{Sr}$ ratios systematically decrease with increasing Ca/Sr ratios (Fig. 6c).

REY concentrations, REY/Si molar ratios, Rb and K con-

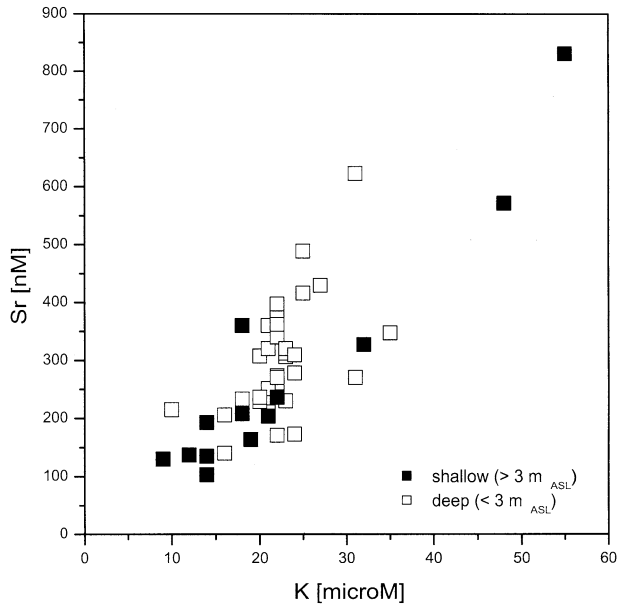


Fig. 5. Graph of dissolved Sr concentration vs. dissolved K concentration in groundwater samples from Cape Cod. Note the positive correlation between Sr and K.

concentrations, and Rb/Si and K/Si molar ratios in well #373 (Appendix 3) increase with increasing depth but show a maximum at ~ 0 m (Fig. 7). This trend is different from that of Sr (and Ca; not shown) concentrations, and Sr/Si and Ca/Si molar ratios (Fig. 7).

REY_{SN} patterns are subparallel for all six groundwater samples (Fig. 8a), increase from the LREE to the HREE ($Nd_{SN}/Yb_{SN} = 0.190.33$), and are characterized by positive Y anomalies ($Y_{SN}/Ho_{SN} = 1.29 - 1.50$) and negative Ce anomalies ($Ce_{SN}/Ce_{SN}^* = 0.53 - 0.73$). The small positive Gd_{SN} anomaly in Figure 8a may indicate the presence of minor amounts of anthropogenic Gd in the groundwater (Bau and Dulski, 1996); however, it does not show up in sediment-normalized REY patterns (Fig. 8b) and we did not investigate this feature any further.

3.2. Bulk Sediment and Mineral Separates

Major and trace element data for the bulk sediment and for the mineral separates are given in Tables 1, 2, and 3; Figure 9 illustrates typical grain shapes and mineral association. Due to its high quartz content, the bulk sediment sample is chemically composed of 95.5% wt. % SiO₂ with minor Al, Fe, K, Na, Ca, and Ti. This suggests a normative mineralogical composition (CIPW-norm calculated following Best, 1982) of quartz (91.6%), K-feldspar (3.6%), albite (2.2%), and rare anorthite (0.18%). The Rb/Sr and the Sr/Eu weight ratio is 1.3 and 118, respectively. The REY_{CN} pattern is close to that of average shale, showing LREE enrichment and a negative Eu_{CN} anomaly (Fig. 10). This chemical composition is in close agreement with the actual mineralogical composition reported for this glaciogenic sediment: 90% quartz, minor plagioclase (5%), and (amongst others) accessory orthoclase, microcline, glauconite, Fe oxides, and mica (e.g., Barber, 1985; Barber et al., 1992;

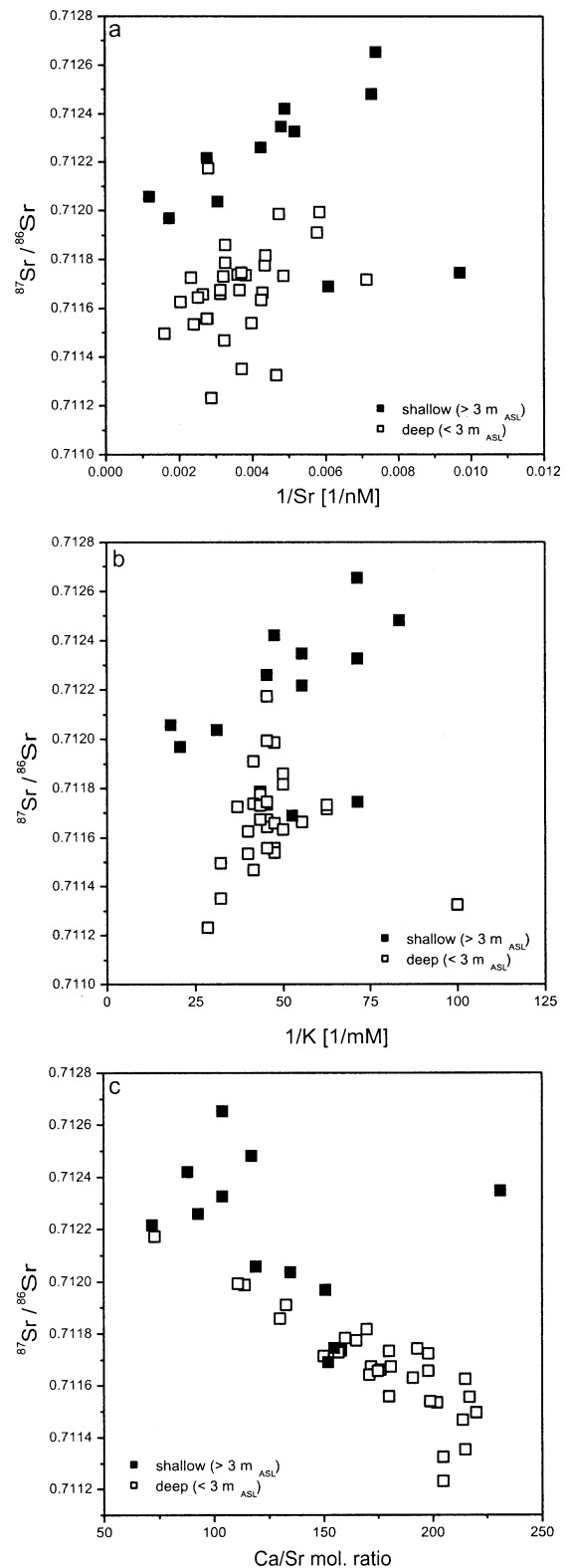


Fig. 6. Graphs of a) $^{87}Sr/^{86}Sr$ vs. $1/[Sr]$, b) $^{87}Sr/^{86}Sr$ vs. $1/[K]$, and c) $^{87}Sr/^{86}Sr$ vs. Ca/Sr mol. ratio. Note the strong trend of decreasing $^{87}Sr/^{86}Sr$ with increasing Ca/Sr molar ratio.

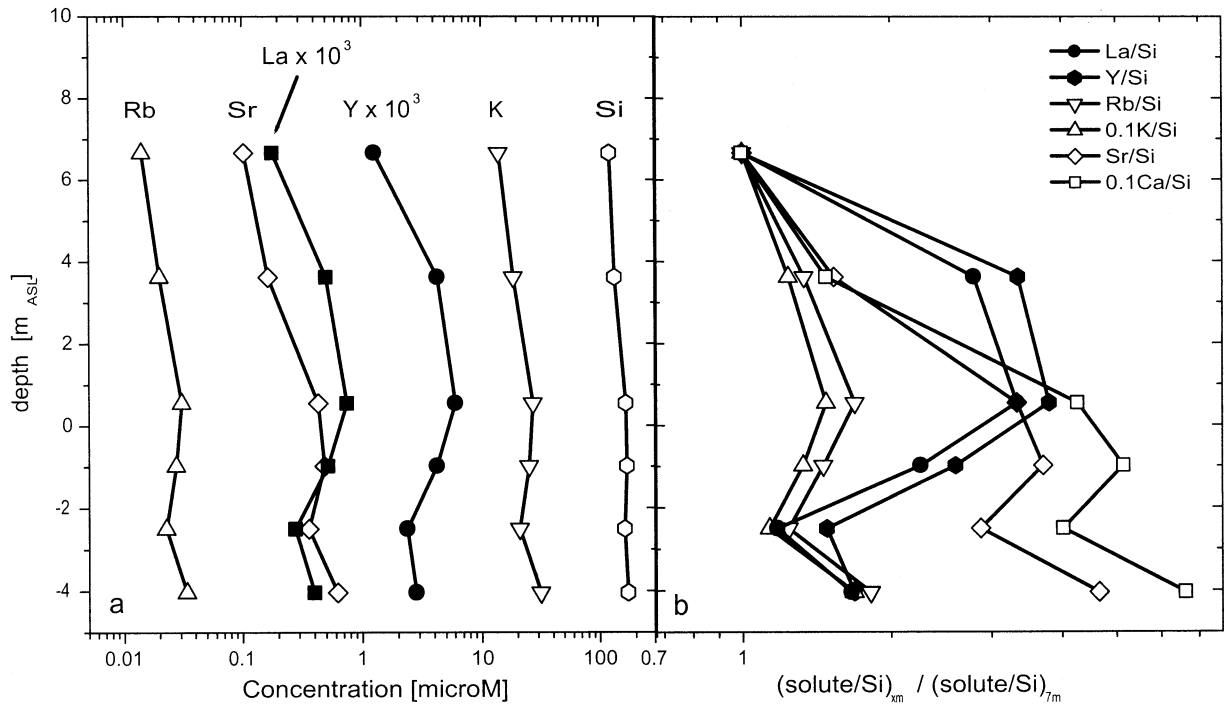


Fig. 7. Graphs of a) dissolved solute concentrations vs. depth in Cape Cod groundwater from well #373, and b) graph of dissolved solute/Si molar ratios normalized to the respective ratio in the uppermost sample (+ 7 m) vs. depth for groundwater from well #373. Note that trends for Y/Si and La/Si are similar to K/Si and Rb/Si, whereas the trends for Ca/Si and Sr/Si are different.

Coston et al., 1995). In a study of nineteen sediment samples from Cape Cod (for which sampling locations and depths are not reported), DeSimone et al. (1997) found somewhat lower

quartz ($62 \pm 14\%$) and higher feldspar contents ($18 \pm 5\%$) than other investigators. Amphibole, glauconite, siderite, and very minor calcite (the latter less than 1% in only half of the

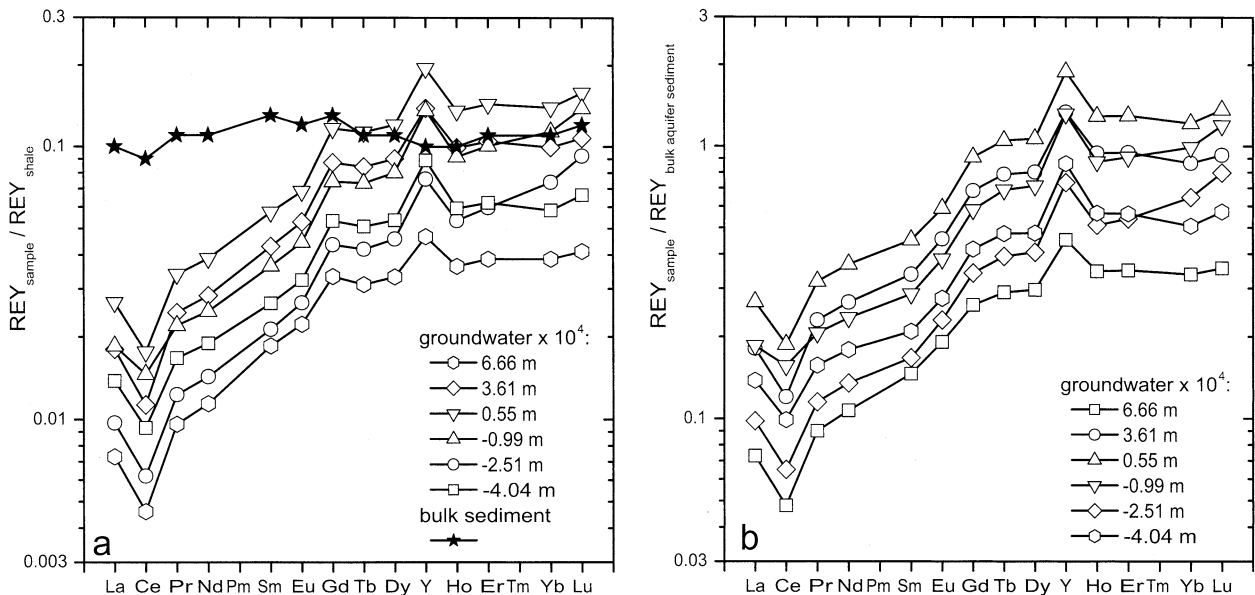


Fig. 8. REY distribution in groundwater from well #373 normalized to a) shale and (b) bulk aquifer sediment. Yttrium is inserted between Dy and Ho according to its effective ionic radius. Note that all patterns are subparallel to each other and show LREE depletion, negative Ce anomalies and positive Y anomalies, but no Eu and La anomalies. The small positive Gd anomalies in the shale-normalized patterns may indicate minor anthropogenic Gd contamination (Bau and Dulski, 1996), but more likely reflect a similar small Gd enrichment in the aquifer sediment.

Table 2. Trace element concentrations ($\mu\text{g kg}^{-1}$) in bulk aquifer sediment, mineral separates, and leaching solutions.

	Bulk ¹	Plag ²	Glauc ³	2 min HCl ⁴	10 min HCl ⁴
Rb	19300	115000	208000	31	38
Sr	14900	508000	213000	53	58
Y	2800	5690	8400	111	160
Zr	36500	70300	71500	<30	<30
Cs	306	1900	2510	2.3	2.8
Ba	93300	101000	104000	742	807
La	3810	18100	17200	80	115
Ce	7490	28300	31900	187	220
Pr	941	3130	3800	20	29
Nd	3590	10600	13700	86	123
Sm	706	1770	2510	19	26
Eu	126	1090	859	3.2	4.7
Gd	595	1360	1900	20	28
Tb	83	195	274	2.8	4.1
Dy	527	1080	1600	16	22
Ho	104	210	308	3.2	4.4
Er	315	634	923	8.8	12
Tm	47	92	140	1.1	1.6
Yb	324	686	934	7.1	9.8
Lu	50	111	144	1.0	1.5
Hf	951	1820	1900	<20	<20
Pb	4410	15300	22000	92	106
Th	1460	3060	4350	5.9	5.5
U	537	1890	1150	4.1	5.3

¹ Bulk sediment, (1) in Table 4

² Plag-rich accessories sample, (5) in Table 4

³ Glauc-rich accessories sample, (6) in Table 4

⁴ Leachates of bulk sediment

samples) were also reported as accessory minerals. Following DeSimone et al. (1997), the clay-sized fraction is composed of illite/mica (49%), kaolinite (26%), mixed-layer illite-smectite (12%), and chlorite (11%). These results (DeSimone et al., 1997) are in broad agreement with those of the previous studies already mentioned, although they document more variability and higher abundance of non-quartz minerals.

The “K-feldspar separate” (2 in Tables 1 and 4) is rich in Si, Al, K, and Na, and its normative mineralogy indicates the presence of quartz, K-feldspar, and minor albite. The “accessories separate” (3 in Table 4) is considerably higher in Al, Fe, Ca, Na, K and Ti, and its normative mineralogy is dominated by quartz and perthite. Microprobe analyses of the “accessories separate” (Table 3) indicate a K-feldspar composition of

Table 3. Electronprobe data for accessories separate 3.

	Plagioclase ¹	Albite ¹	K-spar ²	Mica ²	Glaucinite ²
SiO ₂	61.3	68.5	63.6	45.1	47.6
Al ₂ O ₃	21.9	19.1	19.5	36.1	6.95
CaO	5.25	0.34	nd	nd	0.14
MgO	0.00	nd	nd	1.0	4.52
Na ₂ O	8.50	10.5	0.5	0.8	0.05
K ₂ O	0.11	0.11	14.7	11.1	8.49
Fe ₂ O ₃	0.02	nd	0.1	2.7	19.2
Total	97.0	98.6	98.4	96.8	87.0

¹ Data from Yau (1999)

² Data from this study

nd = not determined

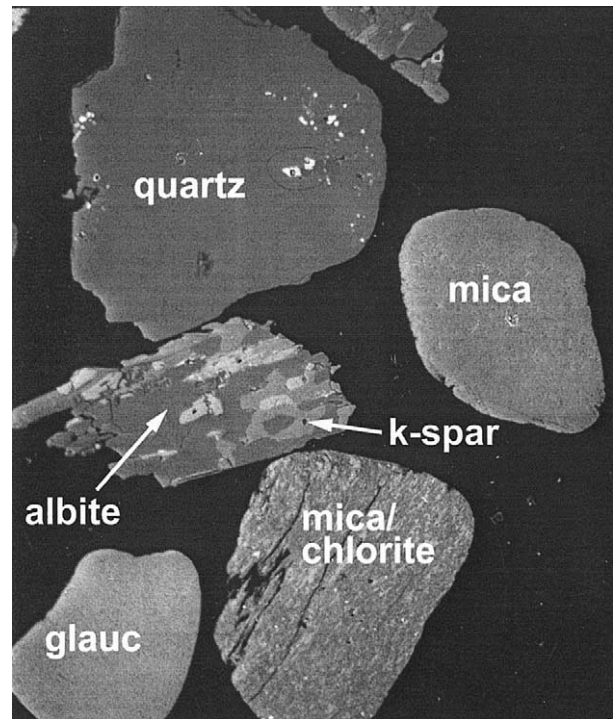


Fig. 9. BSE (back scattered electron) image of “accessories separate” (3 in Tables 1 and 4, prepared as an epoxied grain mount) indicating phases present. Grain size is approximately 0.5–1 mm. Representative compositions are shown in Table 3.

$\text{Ab}_{90}\text{An}_0\text{Or}_{91}$ and an albite composition of $\text{Ab}_{98}\text{An}_2\text{Or}_0$ (composition calculated following Deer et al. (1992)).

The Sr isotopic composition (Fig. 11) of the bulk sediment (Table 4) falls between that of the “K-feldspar separate” (2) and that of the “accessories” separate (3). To elucidate the $^{87}\text{Sr}/^{86}\text{Sr}$ ratios of the K-feldspar and the accessories (Table 4), another fraction of predominantly K-feldspar (4 in Table 4) was hand-picked under the microscope. The $^{87}\text{Sr}/^{86}\text{Sr}$ ratio of this separate 4 documents that K-feldspar dominates the radiogenic Sr component (Fig. 11, Table 4). Two more accessory separates (separates 5 and 6 in Table 4) were also hand-picked and separated using heavy liquids to further concentrate the more mafic minerals. Specifically, in separating these last two fractions, two separate samples of bulk sediment were used and all light colored grains were removed by hand. Bromoform was then used to remove minerals with density $>2.8 \text{ g cm}^{-3}$. One more hand-picking step was used to remove anomalous grains, leaving homogeneous samples that were not combined together but were analyzed separately. Before analysis both samples were thought to be identical and because of lack of sample material only one of these separates (5 in Table 4) was analyzed for Sr isotopes, while both were analyzed for trace elements (Table 2).

Microprobe data (not shown) indicate that separate 5 contains albite ($\text{Ab}_{97}\text{An}_{03}\text{Or}_0$) and small amounts of partly hydrated mica. We did not observe any carbonate minerals. A high abundance of plagioclase in this separate is documented by low Rb and high Sr concentration (115 ppm and 508 ppm, respectively), low Rb/Sr weight ratio (0.23), and, most significant, a positive Eu_{CN} anomaly ($\text{Eu}_{\text{CN}}/\text{Eu}_{\text{CN}}^* = 2.06$, Fig. 10). The Sr

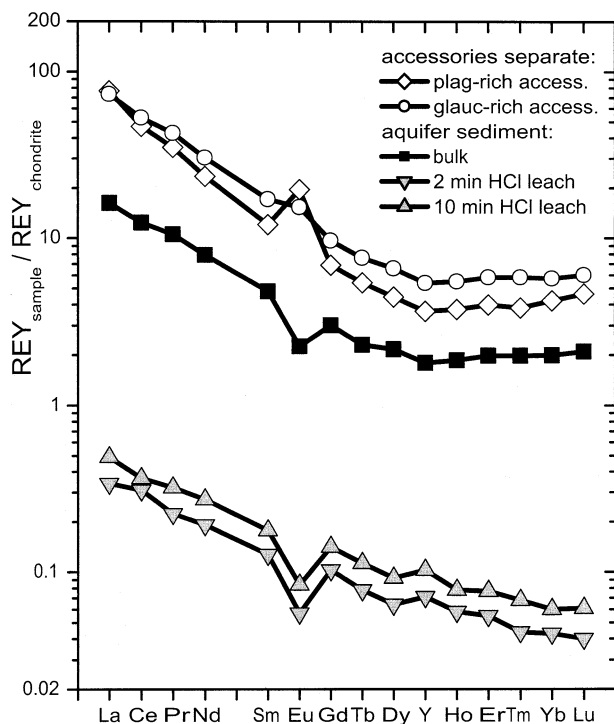


Fig. 10. Chondrite-normalized (C1–chondrite from Anders and Grevesse (1989)) REY patterns of bulk sediment from the Cape Cod aquifer, of a plagioclase-rich and of a glauconite-rich accessory mineral fraction separated from this sediment, and of a 2 min and a 10 min 0.01 mol/L HCl leachate of the bulk sediment. Note that the two leachates show a negative Eu_{CN} anomaly similar in size to that of the bulk sediment, whereas the plagioclase-rich accessories separate shows a positive Eu_{CN} anomaly. Moreover, both leachates show positive Y_{CN} anomalies but no Ce_{CN} anomalies

isotope ratio in this plagioclase-rich accessories separate is very similar to that in the groundwater (Fig. 11).

Separate 6, separated identically as separate 5 but using a different bulk sediment source, shows higher Rb (208 ppm) and lower Sr (213 ppm) concentration than separate 5, a higher Rb/Sr weight ratio (0.98), and only a very small positive Eu_{CN} anomaly ($Eu_{CN}/Eu_{CN}^* = 1.15$, Fig. 10), suggesting that in this separate, Rb-K-bearing minerals such as glauconite are more abundant and that plagioclase is less abundant than in the more plagioclase-rich separate 5. Differences between separates 5

Table 4. $^{87}Sr/^{86}Sr$ ratios of bulk aquifer sediment, mineral separates, and sequential leaching extractions.

	$^{87}Sr/^{86}Sr$
(1) Bulk sediment	0.72017
(2) K-feldspar separate	0.72778
(3) Accessories separate	0.71458
(4) Handpicked K-feldspar sep.	0.74533
(5) Plag-rich accessories separate	0.71149
(6) Glauc-rich accessories separate	nd
Exchangeable extraction	0.71590
Carbonate extraction	0.73356
Fe-Mn-extraction	0.72141

nd = not determined due to lack of sufficient sample

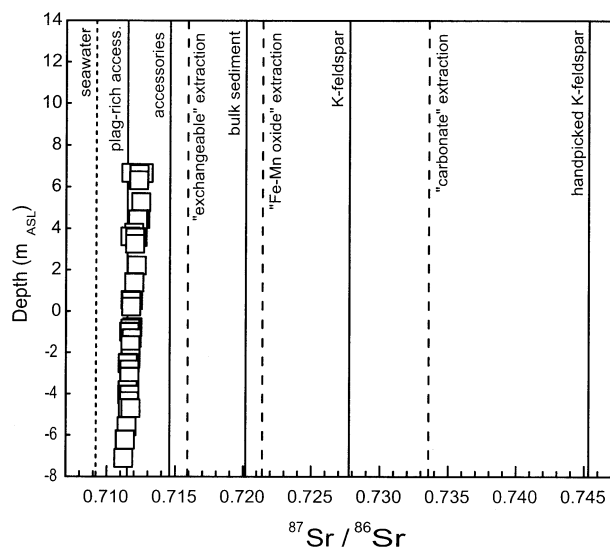


Fig. 11. Graph of the $^{87}Sr/^{86}Sr$ ratio of Cape Cod groundwater vs. depth compared to the $^{87}Sr/^{86}Sr$ ratio of bulk aquifer sediment, mineral separates obtained from it, various leachates produced by sequential leaching of the bulk sediment, and modern seawater. Note similarity of the isotopic composition of Sr in the groundwater and Sr in the plagioclase-rich accessories separate. Rainwater at Cape Cod is inferred to contain Sr of isotopic composition similar to seawater.

and 6 can be attributed to slight differences in the separation procedure or to the mineral abundances in bulk aquifer samples; in the following, these separates are referred to as the “plagioclase-rich accessories” and the “glauconite-rich accessories” separates (5 and 6, respectively, in Table 4). We emphasize that we did not find any carbonate minerals in any of the separates.

3.3. Sequential Extraction and HCl Leaching

All sequential extractions yielded Sr that is more radiogenic than that in the groundwater (Fig. 11). The “exchangeable Sr” is the least radiogenic, whereas the “carbonate extraction” produced the highest $^{87}Sr/^{86}Sr$ ratio; the latter, however, is still less radiogenic than the “handpicked K-feldspar” separate (Fig. 11, Table 4). Since carbonate is absent from the aquifer sediment, the radiogenic Sr leached during the carbonate extraction step may originate from the detrital K-feldspar, K-Rb-rich mica and/or weathering products of K-feldspar and mica, which are the most radiogenic components in the sediment due to their high Rb content. This documents an easily accessible Sr source in the sediment that may release radiogenic Sr even though the host minerals are not dissolved. Preferential release from minerals with more radiogenic $^{87}Sr/^{86}Sr$ compared to less radiogenic $^{87}Sr/^{86}Sr$ is common (Brantley et al., 1998) and well-known from Rb-Sr geochronology (Irber, 1996). Leaching with dilute HCl mobilized only small amounts of Rb and Sr from the sediment (Table 2). Sr is more easily accessible than Rb as shown by the lower Rb/Sr wgt. ratio of 0.6 for the leachates compared to 1.3 for the bulk sediment. These values are considerably higher than the Rb/Sr ratio of the water (0.05 to 0.31).

The REY_{CN} patterns of the leachates show the same negative Eu_{CN} anomaly as the bulk sediment, but are somewhat less

enriched in LREE and depleted in HREE (Fig. 10). The 2 min and 10 min leaching solutions do not show negative Ce_{CN} anomalies, but display small positive Y_{CN} anomalies and show super-chondritic Y/Ho weight ratios of 34.2 and 36.7. In contrast, the bulk sediment shows the “normal” Y/Ho weight ratio of 28.5, which is typical of chondrites, shales, and most igneous rocks (Bau, 1996).

4. DISCUSSION

4.1. Major Cations, Sr and $^{87}Sr/^{86}Sr$

Geochemical modeling using *Geochemist's Workbench* (Bethke, 2002) indicates Cape Cod groundwater sampled for this study is supersaturated with respect to quartz and kaolinite and undersaturated with respect to K-feldspar, albite, and anorthite (thermodynamic dataset based on SUPCRT92 data compilation (Johnson et al., 1991). Quartz remains supersaturated with respect to the groundwater samples even when a higher quartz solubility (Rimstidt, 1997) is used in the model.

The increase of Si, Ca, and Na concentration with depth (Appendix 4) suggests that progressive dissolution of Ca- and Na-bearing silicate minerals exerts an important control on the groundwater composition. The variations of other solute concentrations, such as K, Sr, and Mg (and to some degree Ca) with depth, that do not closely correlate with Si, indicate that ions are exchanging on mineral surfaces, non-silicate phases are dissolving, or Si-conservative alteration reactions are occurring. The latter reactions are most prominently documented in the strong increase of Sr, K, Ca, and Mg concentrations in the shallow part of the aquifer and the concentration spike at +3 m depth (Figs. 3 and 4).

The low $^{87}Sr/^{86}Sr$ ratio of the groundwater contrasts with the high $^{87}Sr/^{86}Sr$ ratio of the aquifer sediment (Fig. 11), which is not unusual. While the bulk sediment shows high $^{87}Sr/^{86}Sr$ due to the high Sr isotopic ratio of the Rb-rich detrital K-feldspar component, the low $^{87}Sr/^{86}Sr$ ratios of the “accessories separate” 3 and, in particular, of the “plagioclase-rich accessories” 5 separate are related to Rb-poor detrital plagioclase and authigenic glauconite. Plagioclase and glauconite are the most abundant Sr-bearing minerals in these separates and progressive dissolution of these accessory minerals appears to control the $^{87}Sr/^{86}Sr$ signature of the Cape Cod groundwater. This is corroborated by the positive correlation between Sr and K (Fig. 5), and between $^{87}Sr/^{86}Sr$ and Sr and K in the shallow part of the aquifer in particular (Fig. 6a and b). All of the above features indicate that plagioclase dissolution alone cannot explain the chemical composition of Cape Cod groundwater.

The decreasing $^{87}Sr/^{86}Sr$ ratio of Cape Cod groundwater with depth clearly shows that plagioclase dissolution is significantly more important in this aquifer than K-feldspar dissolution. This appears to contradict the observation of similar abundance of K-feldspar and plagioclase in the sediments we analyzed. However, many other researchers (e.g., Banfield and Eggleton, 1990; Nesbitt et al., 1997; White et al., 2001) have also observed that, in natural environments even where K-feldspar is more abundant than plagioclase, plagioclase dissolution is faster than that of K-feldspar (for a recent compilation of dissolution rates see, e.g., White et al. (2001)).

The large variation of, for example, K in cation concentration vs. depth plots (Fig. 4) suggests that at least one solute source is inhomogeneously distributed in layers or lenses, particularly in the shallow part of the aquifer. Considering that the solute spike at +3 m depth documents local input of Sr, K, Ca, and Mg, but not of Si (Figs. 3 and 4), congruent dissolution of a silicate phase can be excluded. However, since carbonate minerals are largely absent from the aquifer sediment (Barber et al., 1992; Coston et al., 1995; this study) and dissolution of marine carbonate would not release K to the groundwater, this suggests that the additional solute input exhibited by the spike is accomplished via Si-conservative mineral alteration rather than congruent mineral dissolution. Ion exchange is also an unlikely mechanism, because we see no evidence for loss of ions from solution, but only for gain of ions. Furthermore, the decrease of $^{87}Sr/^{86}Sr$ that accompanies the Sr spike at +3 m depth (Fig. 4b and d) requires that the Sr-contributing mineral be low in radiogenic ^{87}Sr , i.e., it is either low in Rb (and K), or it is too young to have accumulated significant radiogenic ^{87}Sr from the decay of ^{87}Rb . Since “anomalously” high Sr concentrations are accompanied by high K concentrations (Figs. 4b and 5), Sr release from a Rb-K-poor mineral is unlikely. This points to a “young” Rb-K-bearing mineral as solute source, effectively ruling out detrital minerals such as mica or amphibole.

These inferences point toward the accessory authigenic glauconite as an important solute source in the shallow part of the aquifer in addition to plagioclase. Upon weathering, glauconite forms Fe-hydroxides, kaolinite, and mixed-layer clays or smectite (Wolff, 1967; Courbe et al., 1981), which all have been observed within the clay-sized fraction of Cape Cod sediment (Barber, 1985; Yau, 1999). Moreover, during weathering of glauconite, K tends to partition into the solution, producing K-depleted weathering products (Courbe et al., 1981) and K-enriched groundwaters (Wolff, 1967). Weathering of plagioclase also often produces secondary clay minerals (smectites) and/or kaolinite (Proust and Velde, 1978; Rodgers and Holland, 1979; Huang, 1989; Banfield and Eggleton, 1990; Taboada and Garcia, 1999), which also occur in the Cape Cod sediments.

Considering that the Sr in rainwater on Cape Cod should primarily originate from seawater-derived aerosols (Herut et al., 1993; Miller et al., 1993) its isotopic composition should reflect the low $^{87}Sr/^{86}Sr$ ratio of seawater Sr (Fig. 11). The significantly higher $^{87}Sr/^{86}Sr$ ratio of groundwater samples from the uppermost sample ports (Fig. 4d), therefore, indicates that Sr with high $^{87}Sr/^{86}Sr$ ratio is rapidly mobilized as soon as rainwater interacts with the aquifer sediment. This easily accessible Sr is presumed equivalent to the Sr mobilized during the first steps of the sequential leaching experiment, including either or both the “exchangeable Sr” and “carbonate Sr” (Fig. 11). The negative linear correlation between $^{87}Sr/^{86}Sr$ and $1/Sr$ and $1/K$ in the shallow part of the aquifer (Fig. 6) may result from mixing between this easily accessible Sr and the Sr (and K) with low $^{87}Sr/^{86}Sr$ ratio derived from dissolving glauconite and plagioclase.

Assuming that glauconite and plagioclase are the sole sources of cations at depth in the Cape Cod groundwater, cation release observed as a function of depth in the groundwater can constrain model dissolution reactions (Table 5). A general

Table 5. Cation release rate ratios (RRR) for Cape Cod groundwater.

RRR _{<i>i</i>/<i>j</i>}	Calculated from all samples over all depths: moles plag/glauc = 0.86		Calculated from shallow samples (>3m depths): moles plag/glauc = 0.95		Calculated from deep samples (<3m depth): moles plag/glauc = 4.5	
	Observed ¹	Predicted ²	Observed ¹	Predicted ³	Observed ¹	Predicted ⁴
H ⁺ /Si	0.2 ± 0.2	0.3	0.5 ± 0.7	0.58	0.1 ± 0.2	0.12
K/Si	0.04 ± 1.1	0.03	1.1 ± 0.3	0.92	-0.1 ± 0.4	0.003
Na/Si	5.40 ± 0.1	5.30	6.2 ± 0.3	6.14	3.8 ± 0.3	3.80
Ca/Si	0.70 ± 0.1	0.79	1.8 ± 0.3	1.79	0.7 ± 0.3	0.60
Mg/Si	1.30 ± 0.2	1.27	2.8 ± 0.3	2.59	0.1 ± 3.3	0.01
Sr/Si	0.002 ± 0.4	0.01	0.02 ± 0.3	0.01	0.001 ± 0.6	0.005
%[Sr] _{glauc.} ⁶		36%		34%		10%
%[Sr] _{plag.} ⁷		64%		66%		90%

¹ Ratios of observed cation release rates where cation release rate equals slope of regression: all depths ($n = 46$), shallow ($n =$ deep ($n = 33$)).

² Ratios of cation release rates predicted from model dissolution reaction (2).

³ Ratios of cation release rates predicted from model dissolution reaction (3).

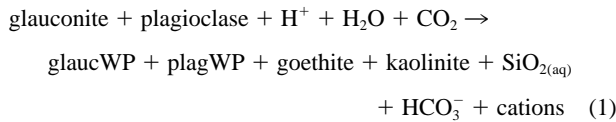
⁴ Ratios of cation release rates predicted from model dissolution reaction (4).

⁵ H⁺ data collected by USGS from same wells and depths sampled in this study (Savoie and LeBlanc, 1998).

⁶ Calculated percentage of moles Sr released from glauconite dissolution in reactions (2), (3), and (4) based upon an assumed glauconite Ca/Sr molar ratio of 312 (Harris, 1982; Courbe et al., 1981).

⁷ Calculated percentage of moles Sr released from plagioclase dissolution in reactions (2), (3), and (4) based upon an assumed plagioclase Ca/Sr molar ratio of 300 (Brantley et al., 1998; Jang and Naslund, 2001; White et al., 2001).

incongruent dissolution reaction consistent with sediment analyses and groundwater chemistry can be written:



where glaucWP and plagWP refer to a glauconite and a plagioclase weathering product, respectively. Consistent with this reaction, all groundwater samples lie within the kaolinite stability field and goethite and kaolinite have been identified in the aquifer (Barber, 1985; Coston et al., 1995; Yau, 1999). We therefore assume that both phases will precipitate regardless of the nature of the glaucWP and plagWP.

Importantly, since release with depth of Na, Ca, Mg, and K are all significant, neither dissolution of glauconite nor plagioclase *alone* can explain the evolution of the groundwater chemistry. Glauconite and plagioclase cannot yield Ca and K, respectively, during dissolution (Table 3). To constrain reaction (1), release rates (RR) and release rate ratios (RRR) can be calculated for Cape Cod groundwater (Table 5):

$$RR_i = \frac{d[i]}{dz} \quad (a)$$

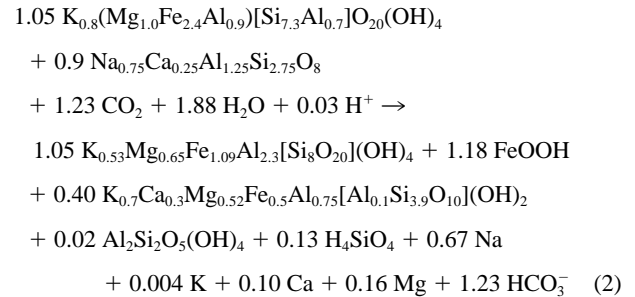
and

$$RRR_{ij} = \frac{RR_i}{RR_j} \quad (b)$$

where $[i]$ and $[j]$ represent the dissolved concentrations of components i and j at depth z .

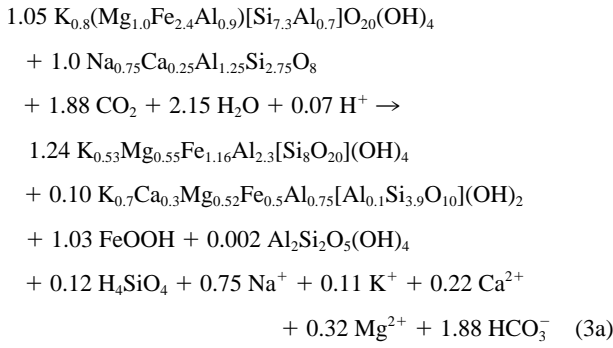
The glaucWP is probably represented by an Fe-rich illite, consistent with weathering products observed by Courbe et al. (1981). The plagWP is inferred to be a smectite, which is consistent with smectite, illite, and kaolinite identified within the clay-sized fraction (<38 μm) of crushed Cape Cod felds-

par. Incorporating these weathering products into reaction (2) predicts cation release consistent with observed RRR (Table 5) over the entire sampled depth:



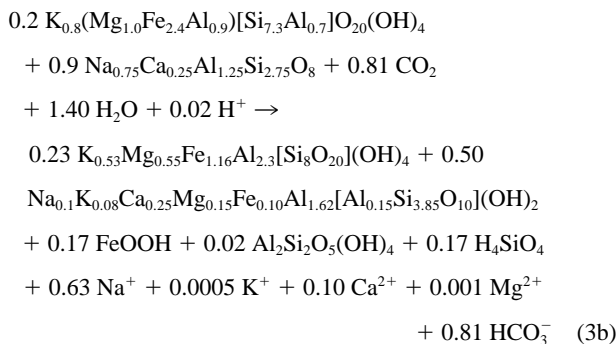
Assuming total Sr released from glauconite and plagioclase goes into solution, Sr/Si ratios (Table 5) can be determined from an inferred Ca/Sr molar ratio in glauconite of 310 (Courbe et al., 1981; Harris, 1982) and a Ca/Sr molar ratio in plagioclase from felsic source rocks of 300 (Brantley et al., 1998; Jang and Naslund, 2001; White et al., 2001). Based upon these calculations, the proportion of Sr released by dissolution of glauconite and plagioclase integrated from depth = 8.3 m to -7.1 m (ASL) is 36 and 64%, respectively (Table 5), and is consistent with extent of dissolution in aquifer water increasing at the rate of 0.06 mol of plagioclase and 0.07 mol of glauconite/m depth.

However, a more careful inspection of Figure 3 reveals that release rate ratios are not constant as a function of depth within the aquifer. RRR are generally higher above +3 m depth; e.g., note the strong increase of dissolved K concentrations in the shallow part compared to the deeper part (Figs. 3 and 4). We infer that the relative contribution of glauconite and plagioclase weathering to cation concentrations in the groundwater changes at about +3 m depth. The following dissolution reaction (3a), with a plagioclase/glaucWP molar dissolution ratio of 0.95) produces cation/Si release ratios as a function of depth within error of those observed in the shallow part of the aquifer:



While similar to Eqn. 2 this dissolution reaction is different as follows: the proportion of plagioclase increases, proton consumption increases, the glaucWP contains less Mg and more Fe, less goethite and kaolinite precipitate, silicic acid production decreases, and the concentrations of Na^+ , K^+ , Ca^{2+} , and Mg^{2+} all increase. [Betts and Grandstaff \(2001\)](#) recently determined a glauconite dissolution rate of $<4.6 \times 10^{-14}$ mol glauconite $\text{m}^{-2} \text{s}^{-1}$ for a field site within the Homers-town Formation, New Jersey, USA. This falls within the range of dissolution rates of plagioclase and K-feldspar reported from field studies ([White et al., 2001](#)), and documents that glauconite, where present, should be an important source of K and other solutes in groundwater as inferred here. Although rich in K and Rb, glauconite typically yields a low $^{87}\text{Sr}/^{86}\text{Sr}$ ratio, because it forms during marine diagenesis at or close to the sediment-water interface and equilibrates with seawater Sr ([Clauer et al., 1992](#)) with an $^{87}\text{Sr}/^{86}\text{Sr}$ ratio of ~ 0.7091 to 0.7092 (e.g., [Clemens et al., 1995](#)). Such a Sr isotopic ratio is close to what is found in the plagioclase-rich accessories separate and in the Cape Cod groundwater ([Fig. 11](#)). Despite the high Rb content, the amount of radiogenic ^{87}Sr in the Cape Cod glauconite can be assumed to be negligible due to its young Pleistocene age. Element input from glauconite that is inhomogeneously distributed in Cape Cod sediment may, therefore, produce enrichment of K and Rb (e.g., in the shallow part of the aquifer), but release Sr that is isotopically very similar to the Sr in the plagioclase minerals.

In marked contrast to the shallow part, K and Mg release rate ratios observed in the deeper part of the aquifer are essentially zero (within error, [Table 5](#)) indicating that for these deeper flow paths, plagioclase weathering dominates cation release to the groundwater. A plagioclase/glauconite molar dissolution ratio of 4.5 produces release rate ratios within error of those observed in the deeper Cape Cod groundwater, based on the following reaction:



In contrast to the shallow weathering reaction this dissolution reaction results in essentially no release of K or Mg to the groundwater. The Sr isotopic composition of Cape Cod groundwater at deeper levels in the aquifer is dominated by Sr released via dissolution from accessory plagioclase, whereas in the shallow part, accessory glauconite is an additional important Sr source.

Hence, we summarize that the Sr budget of the Cape Cod groundwater appears to be affected by an initial rapid input of easily accessible Sr with relatively high $^{87}\text{Sr}/^{86}\text{Sr}$ ratio in the uppermost part of the aquifer. This Sr may be similar to a mixture of the “exchangeable Sr” and the “carbonate Sr” mobilized during the sequential leaching experiment. In the shallow part of the aquifer, additional Sr is derived from dissolving plagioclase and glauconite that contribute K and Sr with lower $^{87}\text{Sr}/^{86}\text{Sr}$ ratio. In the deeper part, Sr input is dominated by dissolving plagioclase and only minor amounts of Sr are derived from dissolving glauconite, resulting in considerably less K input. This decrease in mole flux from dissolving glauconite may be due to either less glauconite at depth or saturation with respect to this phase in the deeper aquifer. Since the isotopic composition of Sr released from plagioclase and glauconite in the Cape Cod aquifer sediments is very similar, the clear separation between the shallow and the deeper part shows up in solute concentrations but not in the Sr isotopic composition.

4.2.1. REY in Cape Cod sediment

Most studies of natural waters suggest that REE patterns are predominantly controlled by complexation in solution and on mineral surfaces available in the aquifer (e.g., [Johannesson and Hendry, 2000](#)) and that dissolution of the source minerals of the REE are of minor importance. Most recently, [Aubert et al. \(2001\)](#) studied the distribution of REE and Sr and Nd isotopes in soils and in creek and spring waters in the Vosges Mts., France. They suggested that apatite and minor plagioclase are the important REE-contributors. However, in most cases, very little is known about REY sources. Notable exceptions are the reducing and acidic hydrothermal black smoker fluids that show positive Eu_{CN} anomalies (e.g., [Michard et al., 1983](#)) often attributed to the breakdown of plagioclase (e.g., [Douville et al., 1999](#)). Such igneous feldspars are usually characterized by positive Eu_{CN} anomalies due to the presence of Eu(II) in the melt and the preferential partitioning of Eu(II) into feldspar during crystallization (e.g., [McKay, 1989](#), and references therein).

Since the Sr isotopic and the major and trace element composition of groundwater from Cape Cod are affected by plagioclase and glauconite dissolution, we tested whether the REY are consistent with this interpretation. The REY distribution in the bulk aquifer sediment from Cape Cod is very similar to that in average shales, although REY concentrations are lower ([Fig. 8a](#)) due to “dilution” by almost REY-free quartz. Assuming a modal abundance of 90% quartz in the bulk sediment with its 3.6 ppm Nd, the Nd content in a hypothetical quartz-free Cape Cod sediment is ~ 32 ppm. This is too high to be hosted by feldspar which is a REY-poor mineral (data for feldspar in [Govindaraju, \(1994\)](#), for example, shows Nd <3 ppm, feldspar from midocean ridge basalts studied by [Douville et al. \(1999\)](#), show less than 0.04 ppm Nd). An even stronger indication

against feldspar as a major REY carrier in Cape Cod sediment is the lack of a positive Eu anomaly in the bulk sediment (Figs. 8a and 10). Hence, the majority of REY in the sediment are hosted by accessories, such as glauconite, mica or apatite. However, as is apparent from Figure 10, the REY-hosting mineral(s) must be LREE-enriched with $La_{CN}/Dy_{CN} > 7$, which rules out LREE-depleted apatite (e.g., Aubert et al., 2001). Published REY data for glauconites with similar K content, i.e., similar degree of maturation (Clauer et al., 1992), vary by more than one order of magnitude and their Nd concentrations range from 1.31 to 27 ppm (Stille and Clauer, 1994; Govindaraju, 1994). Hence, glauconite could be the main REY carrier phase in Cape Cod sediment. Consistent with this inference, the mild leachates are compatible with results from glauconite leaching experiments (Stille and Clauer, 1994).

The mild HCl leachates show REY patterns similar to their parent (Fig. 10), but are slightly HREE-depleted with a small positive Y anomaly. From the Nd in the bulk sediment, 2.4% and 3.4% are leached after 2 and 10 min, respectively, indicating that the REY-hosting phase is partly soluble in dilute HCl. Since only seawater and some marine chemical sediments (and few highly siliceous igneous rocks) may show super-chondritic Y/Ho ratios (Bau, 1996), the easily accessible REY-hosting phase could be glauconite, or a phase associated with the glauconite, that incorporated REY from seawater without major fractionation.

4.2.2. REY in Cape Cod groundwater

REY concentrations in well #373 are at the low end of published data for freshwaters at pH 6 (Johannesson and Hendry, 2000), but consistent with patterns determined in groundwater elsewhere on Cape Cod (E. Sholkovitz, private communication). REY concentrations in well #373 (Fig. 7a) reach a maximum at about +0.5 m depth. Potassium and Rb show similar but less pronounced trends with depth whereas the trend for Sr is somewhat different (Fig. 7a). Solute/Si ratios (in Fig. 7b normalized to the +7 m sample) show parallel trends for the pairs Y and La, K and Rb, and Ca and Sr, respectively. The trends of Y-La and Ca-Sr are significantly different. The discrepancy between the Si-normalized profiles for Ca-Sr and those for Y-La or K-Rb (Fig. 7b) suggests that these elements are derived from different sources, consistent with the inference that plagioclase dissolution does not impact REY concentrations in the groundwater. This interpretation is confirmed by the lack of any positive Eu anomaly in the groundwater (Fig. 8). At low temperature and oxic conditions in the aquifer, Eu occurs as Eu(III), which will not decouple from its trivalent REY neighbors. If the groundwater had received significant REY from feldspar, even REY removal by precipitation or surface-complexation could not have eliminated the positive Eu anomaly.

The similar variation with depth of the REY, K, and Rb in well #373 (Fig. 7) corroborate glauconite as an important source of REY to groundwater. However, the REY patterns provide little direct evidence of their source minerals. Fe-oxide grains and coatings are abundant in Cape Cod sediment and REY scavenging by hydrous Fe- and Mn-oxides is well known to produce positive Y anomalies and depletion of the light REY in the co-existing solution (Bau et al., 1996; Bau, 1999; Ohta

and Kawabe, 2001). While these features could also be due to REY release from glauconite (e.g., Stille and Clauer, 1994) or marine phosphate or carbonate, they cannot be produced by dissolution of other minerals. The negative Ce_{SN} anomalies in Cape Cod groundwater (Fig. 8a) could be due to i) REY input from Ce-depleted minerals, ii) the presence of almost insoluble Ce(IV) compounds in the sediment, or iii) oxidative scavenging of Ce during groundwater migration. The latter explanation is most consistent with the observation that the mild HCl leachates of the bulk sediment do not show the negative Ce anomalies (Fig. 10) expected from dissolution of Ce depleted minerals or from Ce(IV) fixation in the sediment. Moreover, oxidative scavenging of Ce on hydrous Fe oxides has recently been documented experimentally (Bau, 1999). Thus, the presence of Ce anomalies is fully compatible with the high redox-level and the high abundance of Fe oxides. The REY data for the Cape Cod groundwater suggest that source rocks or source minerals do not control or strongly affect the distribution of REE and Y in the groundwater. The REY data for groundwater is thus fully compatible with glauconite as an REY source, although this is not a unique interpretation.

5. CONCLUSIONS

Laboratory experiments indicate that dissolution rates of plagioclase increase with increasing Ca content and that K-feldspar dissolves at a rate similar to that of Na-rich plagioclase (e.g., Blum and Stillings, 1995; White et al., 2001). Hence, it is anticipated that K-feldspar is at least equally important for solute concentrations and Sr isotopic composition of natural waters as plagioclase dissolution. However, dissolution of accessory plagioclase controls the Si- $^{87}Sr/^{86}Sr$ systematics of groundwater despite the Cape Cod aquifer containing both K-feldspar and plagioclase. Besides mineral dissolution reactions, ion exchange with authigenic glauconite may locally generate an additional solute flux into the groundwater. This input does not result in anomalously high $^{87}Sr/^{86}Sr$ ratios, because the post-Pleistocene glauconite is too young to have accumulated significant ^{87}Sr . Hence, the isotopic composition of Sr released from this glauconite reflects that of seawater, and therefore, is similar to that released from dissolving plagioclase. In marked contrast to Si and conservative Sr, the particle-reactive REY in the groundwater cannot be related to dissolving feldspar. Groundwater from Cape Cod lacks a positive Eu anomaly, indicating that plagioclase dissolution does not control its REY budget. This result may be typical of low-temperature natural waters in general. Similarities in the concentration profiles for REY and K-Rb suggest that glauconite may be an important REY-releasing mineral. Hence, it appears that in Cape Cod groundwater, Si and REY are predominantly derived from plagioclase and glauconite, respectively, while Sr is derived from both minerals. Our results indicate that the modal mineralogical composition of an aquifer sediment and its bulk chemical composition do not determine the concentration or isotopic composition of (trace) solutes in related groundwater.

Even in a relatively simple situation such as the Cape Cod aquifer, the study of concentration and isotopic composition of a range of elements showing different geochemical behaviors appears to be a prerequisite for better understanding the different facets of groundwater chemistry. Similar results from a

study of fossil hydrothermal systems that produced economic mineral deposits (Bau et al., 2003) suggest that this may be true for water-rock interaction in general.

Acknowledgments—Doug Kent, Jennifer Coston, Denis LeBlanc, Jennifer Savoie, Kim Bussey, and Matt Gamache of the USGS are acknowledged for data, suggestions, and coordination of field work. The following people are acknowledged for contributions: Simmy Yau (collected MLS waters), Don Voigt (general discussion), and Jim Davis (introduction to the problem). Henry Gong, Shaole Wu, and Mark Angelone of the Materials Characterization Lab (Penn State) helped with ICP-AES, ICP-MS, and electron microprobe analyses respectively. Thanks to J. Ruiz at the University of Arizona for support and access to the W.M. Keck Foundation analytical facility. We thank M. Baker for help in keeping this facility running. Special thanks to the GCA reviewers for their valuable comments and suggestions. This work was funded by Department of Energy grant DE-FG02-95ER14547 to Susan L. Brantley and Carlo G. Pantano, and a Geological Society of America grant to Simmy Yau.

Associate Editor: L. M. Walter

REFERENCES

- Åberg G., Jacks G., and Hamilton P. J. (1989) Weathering rates and $^{87}\text{Sr}/^{86}\text{Sr}$ ratios: an isotopic approach. *Journal of Hydrology* **109**, 65–78.
- Anders E. and Grevesse N. (1989) Abundances of the elements: meteoritic and solar. *Geochim. Cosmochim. Acta* **53**, 197–214.
- Aubert D., Stille P., and Probst A. (2001) REE fractionation during granite weathering and removal by waters and suspended loads: Sr and Nd isotopic evidence. *Geochim. Cosmochim. Acta* **65**, 387–406.
- Banfield J. F. and Eggleton R. A. (1990) Analytical transmission electron microscope studies of plagioclase, muscovite, and K-feldspar weathering. *Clays and Clay Minerals* **38**, 77–89.
- Barber L. B. II (1985) Geochemistry of organic and inorganic compounds in a sewage contaminated aquifer, Cape Cod, Massachusetts. Ph.D dissertation, University of Colorado.
- Barber L. B., II, Thurman E. M., and Runnells D. D. (1992) Geochemical heterogeneity in a sand and gravel aquifer: Effect of sediment mineralogy and particle size on the sorption of chlorobenzenes. *Journal of Contaminant Hydrology* **9**, 35–54.
- Bau M. (1996) Controls on the fractionation of isovalent trace elements in magmatic and aqueous systems: evidence from Y/Ho, Zr/Hf, and lanthanide tetrad effect. *Contributions to Mineralogy and Petrology* **123**, 323–333.
- Bau M. (1999) Scavenging of dissolved yttrium and rare earths by precipitating iron oxyhydroxide: experimental evidence for Ce oxidation, Y-Ho fractionation, and lanthanide tetrad effect. *Geochim. Cosmochim. Acta* **63**, 67–77.
- Bau M. and Dulski P. (1996) Distribution of yttrium and rare-earth elements in the Penge and Kuruman iron-formations, Transvaal Supergroup, South Africa. *Precambrian Research* **79**, 37–55.
- Bau M., Koschinsky A., Dulski P., and Hein J. R. (1996) Comparison of the partitioning behaviours of yttrium, rare earth elements, and titanium between hydrogenetic marine ferromanganese crusts and seawater. *Geochim. Cosmochim. Acta* **60**, 1709–1725.
- Bau M., Romer R. L., Lüders V., and Dulski P. (2003) Tracing element sources of hydrothermal mineral deposits: REE and Y distribution and Sr-Nd-Pb isotopes in fluorite from MVT deposits in the Pennine Orefield, England. *Mineralium Deposita* **38**, 992–1008.
- Bethke C. M. (2002) *The Geochemist's Workbench*. University of Illinois at Urbana-Champaign.
- Betts J. and Grandstaff D. E. (2001) Glauconite dissolution rates and the chemical evolution of vadose waters in the Hornerstown Formation, Hornerstown, New Jersey. *Water-Rock Interaction 2001* 363–366. Abstract Volume.
- Blum A. E. and Stillings L. L. (1995) Feldspar dissolution kinetics. In *Reviews in Mineralogy* (ed. P. H. Ribbe), Vol. 31, pp. 291–351. Mineralogical Society of America.
- Blum J. D., Erel Y., and Brown K. (1993) $^{87}\text{Sr}/^{86}\text{Sr}$ ratios of Sierra Nevada stream waters: implications for relative mineral weathering rates. *Geochim. Cosmochim. Acta* **57**, 5019–5025.
- Blum J. D., Gazis C. A., Jacobson A. D., and Chamberlain C. P. (1998) Carbonate versus silicate weathering in the Raikhot watershed within the High Himalayan Crystalline Series. *Geology* **26**, 411–414.
- Brantley S. L., Chesley J. T., and Stillings L. L. (1998) Isotopic ratios and release rates of strontium measured from weathering feldspars. *Geochim. Cosmochim. Acta* **62**, 1493–1500.
- Bullen T. D., Krabbenhoft D. P., and Kendall C. (1996) Kinetic and mineralogic controls on the evolution of groundwater chemistry and $^{87}\text{Sr}/^{86}\text{Sr}$ in a sandy silicate aquifer, northern Wisconsin, USA. *Geochim. Cosmochim. Acta* **60**, 1807–1821.
- Bullen T. D., White A. F., Blum A. E., Harden J. W., and Schulz M. S. (1997) Chemical weathering of a soil chronosequence on granitoid alluvium: II. Mineralogic and isotopic constraints on the behavior of strontium. *Geochim. Cosmochim. Acta* **61**, 291–306.
- Clauer N., Keppens E., and Stille P. (1992) Sr isotopic constraints on the process of glauconitization. *Geology* **20**, 133–136.
- Clemens S. C., Gromet L. P., and Farrell J. W. (1995) Artefacts in Sr isotope records. *Nature* **373**, 201.
- Clow D. W., Mast M. A., Bullen T. D., and Turk J. T. (1997) Strontium 87/strontium 86 as a tracer of mineral weathering reactions and calcium sources in an alpine/subalpine watershed, Loch Vale, Colorado. *Water Resources Research* **33**, 1335–1351.
- Coston J. A., Fuller C. C., and Davis J. A. (1995) Pb^{2+} and Zn^{2+} adsorption by a natural aluminum-bearing and iron-bearing surface coating on an aquifer sand. *Geochim. Cosmochim. Acta* **59**, 3535–3547.
- Courbe C., Velde B., and Meunier A. (1981) Weathering of glauconites: reversal of the glauconitization process in a soil profile in western France. *Clay Minerals* **16**, 231–243.
- Deer W. A., Howie R. A., and Zussman J. (1992) *An Introduction to the Rock-Forming Minerals*. John Wiley & Sons, Inc, New York.
- DeSimone L. A., Howes B. L., and Barlow P. M. (1997) Mass-balance analysis of reactive transport and cation exchange in a plume of wastewater-contaminated groundwater. *Journal of Hydrology* **203**, 228–249.
- Douville E., Bienvu P., Charlou J. L., Donval J. P., Fouquet Y., Appriou P., and Gamo T. (1999) Yttrium and rare earth elements in fluids from various deep-sea hydrothermal systems. *Geochim. Cosmochim. Acta* **63**, 627–643.
- Dulski P. (1994) Interferences of oxide, hydroxide and chloride analyte species in the determination of rare earth elements in geological samples by inductively coupled plasma-mass spectrometry. *Fresenius J. Anal. Chem.* **350**, 194–203.
- English N. B., Quade J., DeCelles P. G., and Garzzone C. N. (2000) Geologic control of Sr and major element chemistry in Himalayan rivers, Nepal. *Geochim. Cosmochim. Acta* **64**, 2549–2566.
- Govindaraju K. (1994) Compilation of working values and sample description for 383 geostandards. *Geostandards Newsletter* **18**, 158.
- Harris W. B. (1982) Rubidium-strontium glaucony ages, southeastern Atlantic Coastal Plain, USA. In *Numerical Dating in Stratigraphy* (ed. G. S. Odin), pp. 593–606. John Wiley & Sons.
- Herut B., Starinsky A., and Katz A. (1993) Strontium in rainwater from Israel: sources, isotopes and chemistry. *Earth and Planetary Science Letters* **120**, 77–84.
- Huang P. M. (1989) Feldspars, olivines, pyroxenes, and amphiboles. In *Minerals in Soil Environments (Soil Science Society of America Book Series)* (eds. J. B. Dixon and S. B. Weed), pp. 975–1050. Soil Science Society of Amer.
- Irber W. (1996) *Laugungsexperimente an peraluminischen Graniten als Sonde für Alterationsprozesse im finalen Stadium der Granitkristallisation mit Anwendung auf das Rb-Sr-Isotopensystem*. Ph.D dissertation, Free University of Berlin.
- Jacobson A. D. and Blum J. D. (2000) Ca/Sr and $^{87}\text{Sr}/^{86}\text{Sr}$ geochemistry of disseminated calcite in Himalayan silicate rocks from Nanga Parbat: Influence on river-water chemistry. *Geology* **28**, 463–466.
- Jang Y. D. and Naslund H. R. (2001) Major and trace element composition of Skaergaard plagioclase; geochemical evidence for changes in magma dynamics during the final stage of crystallization of the Skaergaard intrusion. *Contributions to Mineralogy and Petrology* **140**, 441–457.

- Johannesson K. H. and Hendry M. J. (2000) Rare earth element geochemistry of groundwaters from a thick till and clay-rich aquitard sequence, Saskatchewan, Canada. *Geochim. Cosmochim. Acta* **64**, 1493–1509.
- Johnson J. W., Oelkers E. H. and Helgeson H. C. (1991) SUPCRT92: A software package for calculating the standard molal thermodynamic properties of minerals, gases, aqueous species and reactions from 1 to 5000 bar and 0° to 1000° C. Earth Sciences Dept., Lawrence Livermore Laboratory, 101 p.
- Johnson T. M. and DePaolo D. J. (1997) Rapid exchange effects on isotope ratios in groundwater systems, 2, Flow investigation using Sr isotope ratios. *Water Resources Research* **33**, 197–209.
- Johnson T. M., Roback R. C., McLing T. L., Bullen T. D., DePaolo D. J., Doughty C., Hunt R. J., Smith R. W., Cecil L. D., and Murrell M. T. (2000) Groundwater “fast paths” in the Snake River Plain aquifer: Radiogenic isotope ratios as natural groundwater tracers. *Geology* **28**, 871–874.
- Kent D. B., Davis J. A., Anderson L. C. D., Rea B. A. and Waite, T. D. (1994) Transport of chromium and selenium in the suboxic zone of a shallow aquifer: Influence of redox and adsorption reactions. *Water Resources Research* **30**, 1099–1114.
- LeBlanc D. R. (1984) Sewage plume in a sand and gravel aquifer, Cape Cod, Massachusetts. In *U.S. Geological Survey Water-Supply Paper Report 2218*, 28.
- LeBlanc D. R., Garabedian S. P., Hess K. M., Gelhar L. W., Quadri R. D., Stollenwerk K. G., and Wood W. W. (1991) Large-scale natural gradient tracer test in sand and gravel, Cape Cod, Massachusetts, 1, Experimental design and observed tracer movement. *Water Resources Research* **27**, 895–910.
- Masterson J. P., Walter D. A. and Savoie J. (1996) Use of particle tracking to improve numerical model calibration and to analyze ground-water flow and contaminant migration, Massachusetts Military Reservation, western Cape Cod, Massachusetts. *U. S. Geological Survey Water-Supply Paper Report 2482*, 50.
- McKay G. A. (1989) Partitioning of rare earth elements between major silicate minerals and basaltic melts. In *Reviews in Mineralogy* (ed. P. H. Ribbe), Vol. 21, pp. 45–77. Mineralogical Society of America.
- McLennan S. M. (1989) Rare earth elements in sedimentary rocks; influence of provenance and sedimentary processes. In *Reviews in Mineralogy* (ed. P. H. Ribbe), Vol. 21, pp. 169–200. Mineralogical Society of America.
- Michard A., Albarede F., Michard G., Minster J. F., and Charlou J. L. (1983) Rare-earth elements and uranium in high-temperature solutions from East Pacific Rise hydrothermal vent field (13 degrees N). *Nature* **303**, 795–797.
- Miller E. K., Blum J. D., and Friedland A. J. (1993) Determination of soil exchangeable-cation loss and weathering rates using Sr isotopes. *Nature* **362**, 438–441.
- Millot R., Gaillardet J., Dupre B., and Allegre C. J. (2002) The global control of silicate weathering rates and the coupling with physical erosion; new insights from rivers of the Canadian Shield. *Earth and Planetary Science Letters* **196**, 83–98.
- Möller P., Dulski P., Gerstenberger H., Morteani G., and Fuganti A. (1998) Rare earth elements, yttrium and H, O, C, Sr, Nd and Pb isotope studies in mineral waters and corresponding rocks from NW-Bohemia, Czech Republic. *Applied Geochemistry* **13**, 975–994.
- Möller P., Dulski P., Bau M., Knappe A., Pekdeger A. and Sommer von Jarmersted C. (2000) Anthropogenic gadolinium as a conservative tracer in hydrology. In *Proceedings of Geofluids III; Third International Conference on Fluid Evolution, Migration and Interaction in Sedimentary Basins and Orogenic Belts* (ed. J. J. Pueyo, E. Cardellach, K. Bitzer and C. Taberner), pp. 409–414, Elsevier.
- Negrel P., Guerrot C., Cocherie A., Azaroual M., Brach M., and Fouillac C. (2000) Rare earth elements, neodymium and strontium isotopic systematics in mineral waters; evidence from the Massif Central, France. *Applied Geochemistry* **15**, 1345–1367.
- Nesbitt H. W., Fedo C. M., and Young G. M. (1997) Quartz and feldspar stability, steady and non-steady-state weathering, and petrogenesis of siliciclastic sands and muds. *Journal of Geology* **105**, 173–191.
- Ohta A. and Kawabe I. (2001) REE(III) adsorption onto Mn dioxide (δ -MnO₂) and Fe oxyhydroxide: Ce(III) oxidation by δ -MnO₂. *Geochim. Cosmochim. Acta* **65**, 695–703.
- Oldale R. N. (1969) Seismic investigations on Cape Cod, Martha's Vineyard and Nantucket, Massachusetts and a topographic map of the basement surface from Cape Cod Bay to the islands. *Geological Survey Research 1969* Chap. B, U. S. Geological Survey. Prof. Pap., Report: P0650-B, pp. B122–B127.
- Probst A., El Gh'mari A., Aubert D., Fritz B., and McNutt R. (2000) Strontium as a tracer of weathering processes in a silicate catchment polluted by acid atmospheric inputs, Strengbach, France. *Chem. Geol.* **170**, 203–219.
- Proust D. and Velde B. (1978) Beidellite crystallization from plagioclase and amphibole precursors; local and long-range equilibrium during weathering. *Clay Minerals* **13**, 199–209.
- Quade J., Roe L., DeCelles P. G., and Ojha T. P. (1997) The late Neogene ⁸⁷Sr/⁸⁶Sr record of lowland Himalayan rivers. *Science* **276**, 1828–1831.
- Rimstidt J. D. (1997) Quartz solubility at low temperatures. *Geochim. Cosmochim. Acta* **61**, 2553–2558.
- Rodgers G. P. and Holland H. D. (1979) Weathering products within microcracks in feldspars. *Geology* **7**, 278–280.
- Savoie J. and LeBlanc D. R. (1998) Water-quality data and methods of analysis for samples collected near a plume of sewage-contaminated ground water, Ashumet Valley, Cape Cod, Massachusetts, 1993–94. *U. S. Geological Survey*, pp. 208. Report: WRI97-4269.
- Shapiro S. D., LeBlanc D., Schlosser P., and Ludin A. (1999) Characterizing a sewage plume using the ³H-³He dating technique. *Ground Water* **37**, 861–878.
- Solomon D. K., Poreda R. J., Cook P. G., and Hunt A. (1995) Site characterization using ³H/³He ground-water ages, Cape Cod, MA. *Ground Water* **33**, 988–996.
- Stille P. and Clauer N. (1994) The process of glauconitization; chemical and isotopic evidence. *Contributions to Mineralogy and Petrology* **117**, 253–262.
- Taboada T. and Garcia C. (1999) Smectite formation produced by weathering in a coarse granite saprolite in Galicia (NW Spain). In *Developments in Micromorphology* (ed. J. J. M. van der Meer and H. J. Muecher), Vol. 35, pp. 281–290, Catena-Verlag Rohdenburg.
- Tessier A., Campbell P. G. C., and Bisson M. (1979) Sequential extraction procedure for the speciation of particulate trace metals. *Analytical Chemistry* **51**, 844–850.
- Thurman E. M., Barber L. B., Jr, and LeBlanc D. R. (1986) Movement and fate of detergents in groundwater: a field study. *Journal of Contaminant Hydrology* **1**, 143–161.
- Tricca A., Stille P., Steinmann M., Kiefel B., Samuel J., and Eikenberg J. (1999) Rare earth elements and Sr and Nd isotopic compositions of dissolved and suspended loads from small river systems in the Vosges Mountains (France), the river Rhine and groundwater. *Chem. Geol.* **160**, 139–158.
- White A. F., Bullen T. D., Schulz M. S., Blum A. E., Huntington T. G., and Peters N. E. (2001) Differential rates of feldspar weathering in granitic regoliths. *Geochim. Cosmochim. Acta* **65**, 847–869.
- Wolff R. G. (1967) X-ray and chemical study of weathering glauconite. *American Mineralogist* **52**, 1129–1138.
- Yau S. (1999) Dissolution kinetics of feldspar in the Cape Cod Aquifer, Massachusetts; calculations of ground water residence times. Master's thesis, The Pennsylvania State University.

APPENDIX 1

Well locations, sampling depths, and select field and USGS data for samples.

Sample #	MLS Well ID	Depth (m) ¹	Latitude (° ' ")	Longitude (° ' ")	Field Data ²			USGS Data ³		
					T (°C)	SpC (μS/cm)	Boron (μg/L)	SpC (μS/cm)	pH	Si (mg/L)
1	262-M01-02GNT	3.79	413713	0703253	8.7	103		95	5.4	3.65
2	262-M01-03RT	-0.78	413713	0703253	9.0	101		94	5.5	4.31
3	262-M01-04BUT	-2.30	413713	0703253	8.8	82		111	5.6	4.59
4	262-M01-05BKT	-3.83	413713	0703253	8.8	76	27.6	110	5.6	4.76
5	508-M01-01PT	6.61	413706	0703256	8.8	93		127	4.9	2.99
6	508-M01-02GNT	3.56	413706	0703256	9.0	109		93	5.1	3.60
7	508-M01-03RT	0.51	413706	0703256	9.4	97		98	5.3	3.86
8	508-M01-04BUT	-1.01	413706	0703256	9.6	125		118	5.3	4.21
9	508-M01-05BKT	-2.54	413706	0703256	9.3	125	28.2	127	5.3	4.52
10	373-M01-01PT	6.66	413703	0703300	10.4	59		71	5.8	3.52
11	373-M01-02GNT	3.61	413703	0703300	9.8	111		131	5.5	4.02
12	373-M01-03RT	0.55	413703	0703300	9.6	137		145	5.6	4.84
13	373-M01-04BUT	-0.99	413703	0703300	9.7	146		145	5.0	4.87
14	373-M01-05BKT	-2.51	413703	0703300	9.8	118		164	5.6	4.89
15	373-M01-06WT	-4.04	413703	0703300	9.7	165	20.7	184	5.6	4.95
16	168-M15-01PT	6.31	413700	0703258	10.2	70		94	4.5	3.06
17	168-M15-02GNT	3.26	413700	0703258	10.0	89		105	5.1	3.53
18	168-M15-03RT	0.22	413700	0703258	10.3	88		70	5.3	4.00
19	168-M15-04BUT	-1.31	413700	0703258	10.4	85		77	5.3	3.94
20	168-M15-05BKT	-2.83	413700	0703258	10.0	85		94	5.3	4.13
21	168-M15-06WT	-4.36	413700	0703258	10.7	89	11.9	91	5.4	4.51
22	442-M01-01PT	6.65	413654	0703303	10.5	73		78	4.7	2.77
23	442-M01-02GNT	3.58	413654	0703303	10.4	62		65	5.2	2.89
24	442-M01-03RT	0.53	413654	0703303	10.6	97		119	5.6	3.52
25	442-M01-04BUT	-1.00	413654	0703303	9.6	128		102	5.7	3.81
26	442-M01-05BKT	-2.53	413654	0703303	8.9	11		85	5.7	3.78
27	442-M01-06WT	-4.06	413654	0703303	8.7	121		92	5.9	3.77
28	442-M01-07O	-5.58	413654	0703303	8.8	118		91	5.8	3.88
29	442-M01-08GY	-7.11	413654	0703303	8.7	116	17.3	104	5.8	4.42
30	471-M01-01PT	4.43	413650	0703304	12.1	67		58	5.2	2.96
31	471-M01-02GNT	1.39	413650	0703304	13.2	87		110	5.5	3.32
32	471-M01-03RT	-1.66	413650	0703304	10.6	123		92	5.6	3.76
33	471-M01-04BUT	-3.19	413650	0703304	11.7	117		76	5.8	3.84
34	471-M01-05BKT	-4.71	413650	0703304	11.5	105		91	5.8	3.96
35	471-M01-06WT	-6.23	413650	0703304	11.8	110	13.2	100	5.8	4.49
36	472-M01-01PT	4.45	413648	0703304	11.6	70		60	5.0	3.31
37	472-M01-02GNT	1.41	413648	0703304	10.4	70		87	5.3	3.40
38	472-M01-03RT	-1.64	413648	0703304	11.7	108		91	5.6	4.10
39	472-M01-04BUT	-3.17	413648	0703304	11.3	124		76	5.7	4.20
40	472-M01-05BKT	-4.69	413648	0703304	11.2	122		84	5.7	4.32
41	472-M01-06WT	-6.21	413648	0703304	10.4	97	14.2	90	5.9	4.70
42	350-M01-01PT	8.30	413646	0703306	11.8	45		61	4.8	2.69
43	350-M01-02GNT	5.26	413646	0703306	10.8	66		80	4.4	2.93
44	350-M01-03RT	2.21	413646	0703306	10.8	65		56	5.1	3.31
45	350-M01-04BUT	-0.84	413646	0703306	11.1	82		110	5.1	4.08
46	350-M01-05BKT	-3.89	413646	0703306	12.1	130	11.7	80	5.4	4.17

¹ Depth relative to average sealevel (ASL)² Data for samples collected on June 5th and 6th, 1997 (this study)³ Data for samples collected by USGS (Savoie and LeBlanc, 1998)

APPENDIX 2
Select ion concentrations [mmol] and $^{87}\text{Sr}/^{86}\text{Sr}$ data.

Sample #	MLS Well ID	[Si]	[Na]	[K]	[Ca]	[Mg]	[Sr] $\times 10^3$	[Al] $\times 10^3$	[Fe] $\times 10^3$	[Mn] $\times 10^3$	[Cl]	[NO ₃]	[SO ₄]	$^{87}\text{Sr}/^{86}\text{Sr}$
1	262-M01-02GNT	0.132	0.305	0.048	0.086	0.119	0.571	1.853	BD	1.092	0.412	0.076	0.108	0.711967
2	262-M01-03RT	0.142	0.518	0.020	0.040	0.113	0.307	1.112	BD	0.546	0.353	0.263	0.070	0.711857
3	262-M01-04BUT	0.142	0.439	0.016	0.037	0.085	0.206	0.371	BD	0.364	BD	BD	BD	0.711732
4	262-M01-05BKT	0.145	0.344	0.021	0.050	0.090	0.251	0.741	BD	0.364	0.223	0.152	0.048	0.711539
5	508-M01-01PT	0.101	0.465	0.018	0.048	0.044	0.208	2.224	BD	1.274	0.432	0.029	0.110	0.712346
6	508-M01-02GNT	0.132	0.375	0.055	0.099	0.155	0.830	1.853	BD	0.546	0.338	0.156	0.132	0.712056
7	508-M01-03RT	0.145	0.505	0.023	0.049	0.124	0.306	2.224	0.537	0.364	0.344	0.194	0.050	0.711784
8	508-M01-04BUT	0.156	0.631	0.022	0.075	0.149	0.378	2.965	0.716	0.182	0.426	0.266	0.060	0.711656
9	508-M01-05BKT	0.163	0.609	0.025	0.084	0.148	0.416	1.483	0.179	0.546	BD	BD	0.178	0.711534
10	373-M01-01PT	0.121	0.311	0.014	0.016	0.064	0.103	0.741	0.179	0.364	0.291	BD	0.066	0.711745
11	373-M01-02GNT	0.133	0.552	0.019	0.025	0.095	0.164	1.112	0.179	0.546	BD	BD	0.198	0.711689
12	373-M01-03RT	0.166	0.565	0.027	0.085	0.215	0.429	2.595	0.716	0.546	BD	BD	0.276	0.711724
13	373-M01-04BUT	0.170	0.561	0.025	0.105	0.237	0.488	2.595	0.895	0.364	1.165	BD	0.232	0.711624
14	373-M01-05BKT	0.161	0.548	0.021	0.078	0.144	0.360	2.224	0.716	0.546	0.310	0.376	0.056	0.711555
15	373-M01-06WT	0.172	0.713	0.031	0.137	0.220	0.622	1.483	0.537	0.546	0.384	0.879	0.032	0.711495
16	168-M15-01PT	0.108	0.305	0.014	0.020	0.048	0.193	BD	BD	1.092	0.319	BD	0.102	0.712325
17	168-M15-02GNT	0.112	0.452	0.032	0.044	0.092	0.327	1.853	0.537	0.546	0.477	0.029	0.074	0.712036
18	168-M15-03RT	0.140	0.428	0.023	0.038	0.113	0.230	0.741	0.179	0.364	0.423	0.068	0.040	0.711774
19	168-M15-04BUT	0.147	0.470	0.020	0.039	0.106	0.229	3.336	1.253	0.546	0.319	0.110	0.046	0.711816
20	168-M15-05BKT	0.147	0.435	0.018	0.041	0.097	0.233	0.741	0.179	0.364	0.333	0.119	0.056	0.711662
21	168-M15-06WT	0.165	0.500	0.020	0.045	0.092	0.236	0.371	0.179	0.910	0.313	0.092	0.076	0.711631
22	442-M01-01PT	0.101	0.291	0.014	0.014	0.029	0.135	BD	BD	0.910	0.327	BD	0.092	0.712652
23	442-M01-02GNT	0.106	0.309	0.018	0.026	0.046	0.360	4.448	0.179	0.910	0.305	BD	0.076	0.712215
24	442-M01-03RT	0.120	0.605	0.024	0.023	0.086	0.173	1.112	BD	0.546	0.505	0.047	0.086	0.711910
25	442-M01-04BUT	0.134	0.766	0.024	0.044	0.114	0.278	0.741	0.358	0.364	0.575	0.160	0.054	0.711736
26	442-M01-05BKT	0.140	0.679	0.022	0.047	0.110	0.273	0.371	BD	0.364	0.570	0.097	0.056	0.711673
27	442-M01-06WT	0.147	0.561	0.023	0.058	0.118	0.320	2.224	0.716	0.364	0.595	BD	0.032	0.711674
28	442-M01-07O	0.147	0.631	0.024	0.066	0.110	0.309	1.112	0.537	0.364	0.598	BD	0.042	0.711466
29	442-M01-08GY	0.182	0.587	0.035	0.071	0.100	0.347	1.483	0.358	0.546	0.485	0.081	0.046	0.711230
30	471-M01-01PT	0.111	0.384	0.022	0.022	0.045	0.236	8.154	BD	1.092	0.358	BD	0.072	0.712258
31	471-M01-02GNT	0.116	0.552	0.022	0.019	0.072	0.171	1.112	0.537	0.364	0.451	BD	0.078	0.711992
32	471-M01-03RT	0.142	0.687	0.023	0.049	0.117	0.312	1.483	0.537	0.364	0.525	0.240	0.046	0.711729
33	471-M01-04BUT	0.141	0.483	0.021	0.056	0.121	0.320	0.741	0.358	0.182	0.564	0.063	0.036	0.711657
34	471-M01-05BKT	0.176	0.631	0.022	0.052	0.098	0.270	BD	6.804	0.546	0.575	0.060	0.029	0.711743
35	471-M01-06WT	0.163	0.587	0.031	0.058	0.087	0.270	1.853	0.895	0.364	0.516	0.102	0.028	0.711351
36	472-M01-01PT	0.118	0.359	0.021	0.018	0.046	0.204	BD	1.253	2.548	0.370	BD	0.058	0.712418
37	472-M01-02GNT	0.111	0.315	0.021	0.024	0.064	0.211	1.853	0.537	0.546	0.375	BD	0.068	0.711986
38	472-M01-03RT	0.139	0.561	0.022	0.041	0.109	0.261	1.853	0.179	0.364	0.516	0.084	0.046	0.711733
39	472-M01-04BUT	0.147	0.587	0.022	0.068	0.146	0.397	1.483	0.358	0.364	0.623	0.068	0.029	0.711643
40	472-M01-05BKT	0.147	0.596	0.022	0.065	0.117	0.362	1.112	0.179	0.364	0.609	0.063	0.048	0.711557
41	472-M01-06WT	0.159	0.531	0.010	0.044	0.068	0.215	1.483	0.358	0.182	0.471	0.050	0.042	0.711324
42	350-M01-01PT	0.095	0.174	0.009	0.009	0.032	0.130	BD	0.358	0.546	0.124	BD	0.060	NA
43	350-M01-02GNT	0.101	0.271	0.012	0.016	0.037	0.137	BD	BD	1.274	0.372	BD	0.052	0.712481
44	350-M01-03RT	0.113	0.291	0.022	0.026	0.060	0.356	1.483	0.179	0.364	0.307	BD	0.078	0.712172
45	350-M01-04BUT	0.126	0.452	0.016	0.021	0.060	0.140	0.741	0.358	0.364	0.384	BD	0.074	0.711715
46	350-M01-05BKT	0.150	0.626	0.022	0.059	0.127	0.340	BD	0.179	0.364	0.505	0.250	0.044	NA

BD = below detection limits; NA = not analyzed

APPENDIX 3Concentrations of Sr, Rb, Y, and REE in 0.45 μm -filtered groundwater from MLS well #373.

Sample port	PT (+6.66 m)	GNT (+3.61 m)	RT (+0.55 m)	BUT (-0.99 m)	BKT (-2.57 m)	WT (-4.04 m)
Rb	14.16	19.95	30.66	27.62	22.77	33.80
Sr	102.7	166.4	478.1	507.6	366.5	663.5
Y	1.419	4.197	5.913	4.124	2.306	2.707
La	0.201	0.496	0.735	0.508	0.268	0.379
Ce	0.259	0.640	1.002	0.832	0.352	0.527
Pr	0.060	0.154	0.212	0.138	0.077	0.105
Nd	0.267	0.665	0.911	0.584	0.336	0.445
Sm	0.068	0.159	0.212	0.135	0.079	0.098
Eu	0.016	0.038	0.049	0.032	0.019	0.023
Gd	0.099	0.259	0.345	0.220	0.129	0.158
Tb	0.015	0.041	0.055	0.036	0.020	0.025
Dy	0.096	0.260	0.345	0.231	0.132	0.154
Ho	0.022	0.059	0.081	0.055	0.032	0.036
Er	0.066	0.178	0.244	0.171	0.102	0.106
Tm*	nr	nr	nr	nr	nr	nr
Yb	0.063	0.162	0.227	0.185	0.121	0.095
Lu	0.010	0.027	0.039	0.034	0.023	0.016

All concentrations in nM; *Tm concentrations are not reported (nr), because a Tm spike was used to determine the element yield after preconcentration; sampling port depth is relative to average sea level.

APPENDIX 4Concentration change with depth [$\mu\text{M m}^{-1}$].

	Si	Na	K	Ca	Mg	Sr
Shallow part	3.373	55.16	4.563	6.944	11.91	0.039
Deeper part	7.403	31.76	1.395	4.828	4.292	0.001
Complete profile	5.646	26.80	1.687	4.023	4.413	0.014